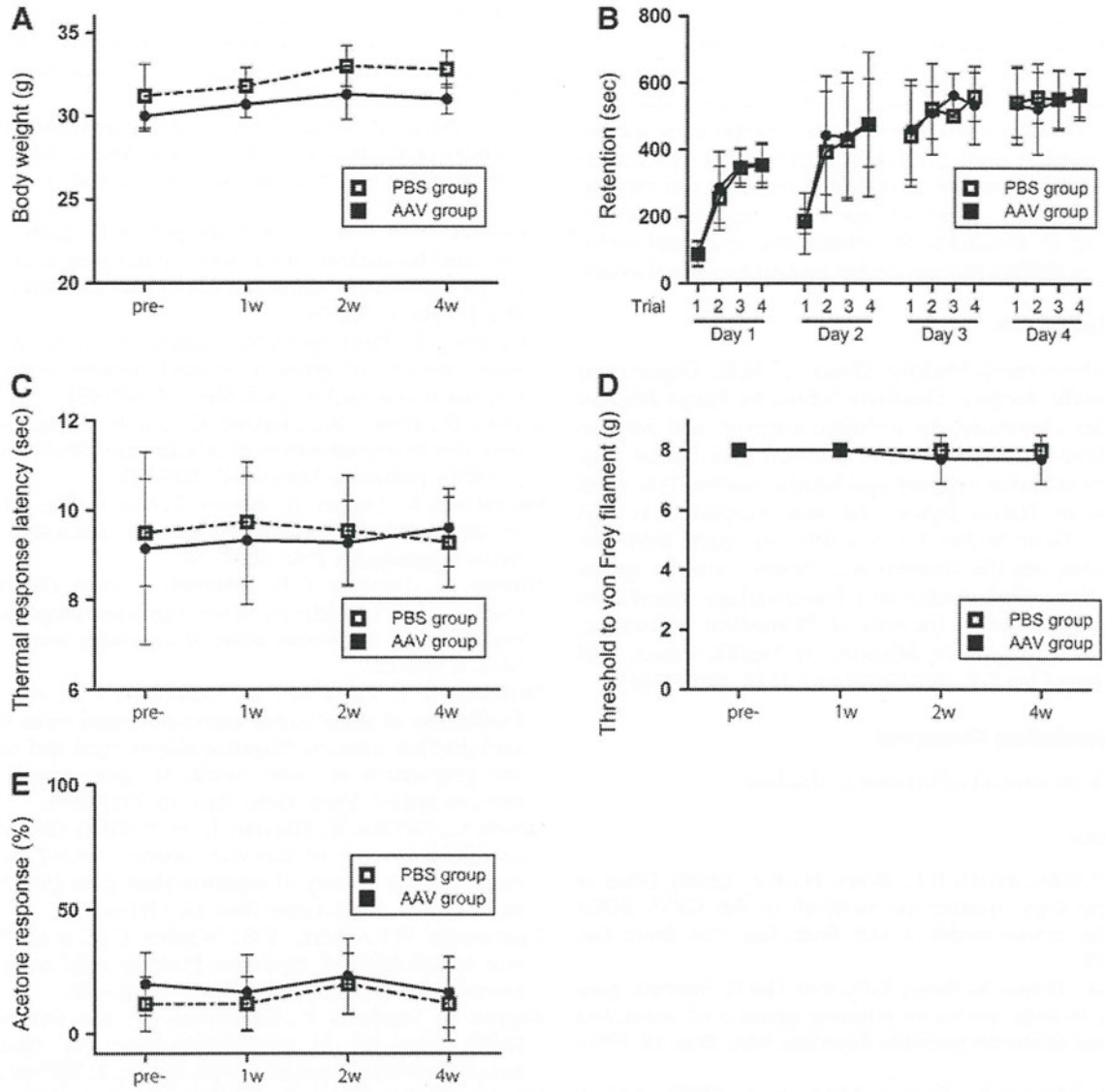

FIG. 4. Assessment of body weight, locomotion, and plantar sensation in the hind limbs of PBS- and AAV-treated mice. **(A)** Throughout the 4-week experimental period, body weight remained similar in PBS- and AAV-treated mice. Data are presented as means ± 1 SD ($n = 6$ mice per group; $p > 0.05$). **(B)** In the accelerating Rotarod test performed 4 weeks after injection, all mice in both the PBS- and AAV-treated groups demonstrated similar performance levels. Each mouse was trained in four trials daily for a total of 4 days. Data are presented as means ± 1 SD ($n = 6$ mice per group; $p > 0.05$). **(C)** Latency of response to heat stimulation, **(D)** threshold for von Frey filaments, and **(E)** response to acetone application. No significant differences were observed between the PBS- and AAV-treated groups. Data are represented as means ± 1 SD ($n = 6$ mice per group; $p > 0.05$).

and achieve long-term suppression of target gene expression in the CNS.

In general, intrathecal injection of a viral vector is a safe, minimally invasive, and sound approach (Sakura *et al.*, 1996; Pogatzki *et al.*, 2000). Using this route with AAV vector, we showed that target gene mRNA expression was not decreased in cardiac and skeletal muscles or liver. Therefore, intrathecally injected AAV9 likely remains localized within, and is specific for, the CNS. Moreover, through the use of intensive motor and sensory behavioral tests, we confirmed the lack of adverse effect associated with this method. Our study showed that intrathecal administration of an AAV9-based vector does not damage the tissues histologically or alter the expression of unrelated endogenous mRNAs in the spinal cord and DRG. Thus, we consider that intrathecal injection of shRNA-AAV9 is sufficiently safe for clinical application.

For the treatment of diseases causing intractable pain, intrathecally administered siRNA had been used to target molecules such as the δ opioid receptor (Luo *et al.*, 2005), TRPV1 (Christoph *et al.*, 2006), and the NR1 (Garraway *et al.*, 2009) and NR2B (Tan *et al.*, 2005) subunits of the *N*-methyl-D-aspartic acid receptor in the spinal cord or DRG. Similarly, the intrathecal shRNA-AAV9 approach might be used as therapy for pathological states in which central molecular integrators of nociceptive or pain-related receptors are activated, such as Sjögren's neuropathy (Pavlakis *et al.*, 2011), complex regional pain syndrome (Wei *et al.*, 2009), cancer pain (Pan *et al.*, 2010), and the hypersensitivity of sensory

neurons involved in chronic neuropathic pain (Luo *et al.*, 2005; Christoph *et al.*, 2006; Garraway *et al.*, 2009).

To our knowledge, our study is the first to demonstrate that intrathecal injection of AAV9 vector encoding shRNA is safe and effective for the suppression of target gene expression in the spinal cord and DRG of mice. Although further investigations are needed to optimize the dose and components of the vector construct, our study represents an important step in advancing the clinical use of a viral vector encoding an shRNA as a promising system for gene therapy.

Acknowledgments

The authors thank Madoka Ukegawa, M.D., Department of Orthopedic Surgery, Graduate School of Tokyo Medical and Dental University, for technical support, and Miyoko Ojima, Graduate School, Tokyo Medical and Dental University, for technical support and helpful advice. This work was done in Tokyo, Japan, and was supported in part through a Grant-in-Aid for Scientific Research from the Japan Society for the Promotion of Science and by grants from the Japan Orthopedics and Traumatology Foundation (no. 217), the National Institute of Biomedical Innovation, Japan (to T.Y.), and the Ministry of Health, Labor, and Welfare, Japan (to T.Y. [#2212070] and H.M. [#2212148]).

Author Disclosure Statement

There is no conflict of interest to disclose.

References

Alexander, G.M., Erwin, K.L., Byers, N., *et al.* (2004). Effect of transgene copy number on survival in the G93A SOD1 transgenic mouse model of ALS. Brain Res. Mol. Brain Res. 130, 7–15.

Bevan, A.K., Duque, S., Foust, K.D., *et al.* (2011). Systemic gene delivery in large species for targeting spinal cord, brain, and peripheral tissues for pediatric disorders. Mol. Ther. 19, 1971–1980.

Bish, L.T., Morine, K., Sleeper, M.M., *et al.* (2008). Adeno-associated virus (AAV) serotype 9 provides global cardiac gene transfer superior to AAV1, AAV6, AAV7, and AAV8 in the mouse and rat. Hum. Gene Ther. 19, 1359–1368.

Christoph, T., Grünweller, A., Mika, J., *et al.* (2006). Silencing of vanilloid receptor TRPV1 by RNAi reduces neuropathic and visceral pain *in vivo*. Biochem. Biophys. Res. Commun. 350, 238–243.

Christoph, T., Bahrenberg, G., De Vry, J., *et al.* (2008). Investigation of TRPV1 loss-of-function phenotypes in transgenic shRNA expressing and knockout mice. Mol. Cell. Neurosci. 37, 579–589.

Dorn, G., Patel, S., Wotherspoon, G., *et al.* (2004). siRNA relieves chronic neuropathic pain. Nucleic Acids Res. 32, e49.

Federici, T., Taub, J.S., Baum, G.R., *et al.* (2011). Robust spinal motor neuron transduction following intrathecal delivery of AAV9 in pigs. Gene Ther. 15. doi: 10.1038/gt.2011.130.

Fire, A., Xu, S., Montgomery, M.K., *et al.* (1998). Potent and specific genetic interference by double-stranded RNA in *Caenorhabditis elegans*. Nature 391, 806–811.

Fu, H., Muenzer, J., Samulski, R.J., *et al.* (2003). Self-complementary adeno-associated virus serotype 2 vector: Global distribution and broad dispersion of AAV-mediated transgene expression in mouse brain. Mol. Ther. 8, 911–917.

Fu, H., Dirosario, J., Killedar, S., *et al.* (2011). Correction of neurological disease of mucopolysaccharidosis IIIB in adult mice by rAAV9 trans-blood–brain barrier gene delivery. Mol. Ther. 19, 1025–1033.

Fu, Y., Zhang, Q., Kang, C., *et al.* (2009). Inhibitory effects of adenovirus mediated COX-2, Akt1 and PIK3R1 shRNA on the growth of malignant tumor cells *in vitro* and *in vivo*. Int. J. Oncol. 35, 583–591.

Garraway, S.M., Xu, Q., and Inturrisi, C.E. (2009). siRNA-mediated knockdown of the NR1 subunit gene of the NMDA receptor attenuates formalin-induced pain behaviors in adult rats. J. Pain 10, 380–390.

Gregorevic, P., Blankinship, M.J., Allen, J.M., *et al.* (2004). Systemic delivery of genes to striated muscles using adeno-associated viral vectors. Nat. Med. 10, 828–834.

Grimm, D., Streetz, K.L., Jopling, C.L., *et al.* (2006). Fatality in mice due to oversaturation of cellular microRNA/short hairpin RNA pathways. Nature 441, 537–541.

Hargreaves, K., Dubner, R., Brown, F., *et al.* (1988). A new and sensitive method for measuring thermal nociception in cutaneous hyperalgesia. Pain 32, 77–88.

Hassani, Z., Lemkine, G.F., Erbacher, P., *et al.* (2005). Lipid-mediated siRNA delivery down-regulates exogenous gene expression in the mouse brain at picomolar levels. J. Gene Med. 7, 198–207.

Hermens, W.T., Ter Brake, O., Dijkhuizen, P.A., *et al.* (1999). Purification of recombinant adeno-associated virus by iodixanol gradient ultracentrifugation allows rapid and reproducible preparation of vector stocks for gene transfer in the nervous system. Hum. Gene Ther. 10, 1885–1891.

Janson, C., McPhee, S., Bilaniuk, L., *et al.* (2002). Clinical protocol: Gene therapy of Canavan disease: AAV-2 vector for neurosurgical delivery of aspartoacylase gene (ASPA) to the human brain. Hum. Gene Ther. 13, 1391–1412.

Kaemmerer, W.F., Reddy, R.G., Warlick, C.A., *et al.* (2000). *In vivo* transduction of cerebellar Purkinje cells using adeno-associated virus vectors. Mol. Ther. 2, 446–457.

Kappel, S., Matthess, Y., Kaufmann, M., and Strebhardt, K. (2007). Silencing of mammalian genes by tetracycline-inducible shRNA expression. Nat. Protoc. 2, 3257–3269.

Kawase, M., Murakami, K., Fujimura, M., *et al.* (1999). Exacerbation of delayed cell injury after transient global ischemia in mutant mice with CuZn superoxide dismutase deficiency. Stroke 30, 1962–1968.

Li, G., Li, D., Xie, Q., *et al.* (2008). RNA interfering connective tissue growth factor prevents rat hepatic stellate cell activation and extracellular matrix production. J. Gene Med. 10, 1039–1047.

Luo, M.C., Zhang, D.Q., Ma, S.W., *et al.* (2005). An efficient intrathecal delivery of small interfering RNA to the spinal cord and peripheral neurons. Mol. Pain 1, 29.

Manno, C.S., Pierce, G.F., Arruda, V.R., *et al.* (2006). Successful transduction of liver in hemophilia by AAV-Factor IX and limitations imposed by the host immune response. Nat. Med. 12, 342–347.

Marks, W.J., Ostrem, J.L., Verhagen, L., *et al.* (2008). Safety and tolerability of intraputaminal delivery of CERE-120 (adeno-associated virus serotype 2-neurturin) to patients with idiopathic Parkinson's disease: An open-label, phase I trial. Lancet Neurol. 7, 400–408.

Mayra, A., Tomimitsu, H., Kubodera, T., *et al.* (2011). Intraperitoneal AAV9-shRNA inhibits target expression in neonatal skeletal and cardiac muscles. Biochem. Biophys. Res. Commun. 405, 204–209.

Mikami, M., and Yang, J. (2005). Short hairpin RNA-mediated selective knockdown of NaV1.8 tetrodotoxin-resistant voltage-gated sodium channel in dorsal root ganglion neurons. Anesthesiology 103, 828–836.

Mitchell, M., Jerebtsova, M., Batshaw, M.L., *et al.* (2000). Long-term gene transfer to mouse fetuses with recombinant adenovirus and adeno-associated virus (AAV) vectors. Gene Ther. 7, 1986–1992.

Pan, H.L., Zhang, Y.Q., and Zhao, Z.Q. (2010). Involvement of lysophosphatidic acid in bone cancer pain by potentiation of TRPV1 via PKCε pathway in dorsal root ganglion neurons. Mol. Pain 6, 85.

Pavlakis, P.P., Alexopoulos, H., Kosmidis, M.L., *et al.* (2011). Peripheral neuropathies in Sjögren syndrome: A new reappraisal. J. Neurol. Neurosurg. Psychiatry 82, 798–802.

Peden, C.S., Burger, C., Muzyczka, N., and Mandel, R.J. (2004). Circulating anti-wild-type adeno-associated virus type 2 (AAV2) antibodies inhibit recombinant AAV2 (rAAV2)-mediated, but not rAAV5-mediated, gene transfer in the brain. J. Virol. 78, 6344–6359.

Pogatzki, E.M., Zahn, P.K., and Brennan, T.J. (2000). Lumbar catheterization of the subarachnoid space with a 32-gauge polyurethane catheter in the rat. Eur. J. Pain 4, 111–113.

Puskovic, V., Wolfe, D., Goss, J., *et al.* (2004). Prolonged biologically active transgene expression driven by HSV LAP2 in brain *in vivo*. Mol. Ther. 10, 67–75.

Reaume, A.G., Elliott, J.L., Hoffman, E.K., *et al.* (1996). Motor neurons in Cu/Zn superoxide dismutase-deficient mice develop normally but exhibit enhanced cell death after axonal injury. Nat. Genet. 13, 43–47.

Rodriguez-Lebron, E., Denovan-Wright, E.M., Nash, K., *et al.* (2005). Intrastriatal rAAV-mediated delivery of anti-huntingtin shRNAs induces partial reversal of disease progression in R6/1 Huntington's disease transgenic mice. Mol. Ther. 12, 618–633.

Rossi, J.J. (2008). Expression strategies for short hairpin RNA interference triggers. Hum. Gene Ther. 19, 313–317.

Saito, Y., Yokota, T., Mitani, T., *et al.* (2005). Transgenic small interfering RNA halts amyotrophic lateral sclerosis in a mouse model. J. Biol. Chem. 280, 42826–42830.

Sakura, S., Hashimoto, K., Bollen, A.W., *et al.* (1996). Intrathecal catheterization in the rat: Improved technique for morphologic analysis of drug-induced injury. Anesthesiology 85, 1184–1189.

Senechal, Y., Kelly, P.H., Cryan, J.F., *et al.* (2007). Amyloid precursor protein knockdown by siRNA impairs spontaneous alternation in adult mice. J. Neurochem. 102, 1928–1940.

Senn, C., Hangartner, C., Moes, S., *et al.* (2005). Central administration of small interfering RNAs in rats: A comparison with antisense oligonucleotides. Eur. J. Pharmacol. 522, 30–37.

Snyder, B.R., Gray, S.J., Quach, E.T., *et al.* (2011). Comparison of adeno-associated viral vector serotypes for spinal cord and motor neuron gene delivery. Hum. Gene Ther. 22, 1129–1135.

Storek, B., Reinhardt, M., Wang, C., *et al.* (2008). Sensory neuron targeting by self-complementary AAV8 via lumbar puncture for chronic pain. Proc. Natl. Acad. Sci. U.S.A. 105, 1055–1060.

Tan, P.H., Yang, L.C., Shih, H.C., *et al.* (2005). Gene knockdown with intrathecal siRNA of NMDA receptor NR2B subunit reduces formalin-induced nociception in the rat. Gene Ther. 12, 59–66.

Towne, C., Raoul, C., Schneider, B.L., and Aebischer, P. (2008). Systemic AAV6 delivery mediating RNA interference against SOD1: Neuromuscular transduction does not alter disease progression in fALS mice. Mol. Ther. 16, 1018–1025.

Uno, Y., Piao, W., Miyata, K., *et al.* (2011). High-density lipoprotein facilitates *in vivo* delivery of α-tocopherol-conjugated short-interfering RNA to the brain. Hum. Gene Ther. 22, 711–719.

Wei, T., Li, W.W., Guo, T.Z., *et al.* (2009). Post-junctional facilitation of substance P signaling in a tibia fracture rat model of complex regional pain syndrome type I. Pain 144, 278–286.

Worgall, S., Sondhi, D., Hackett, N.R., *et al.* (2008). Treatment of late infantile neuronal ceroid lipofuscinosis by CNS administration of a serotype 2 adeno-associated virus expressing CLN2 cDNA. Hum. Gene Ther. 19, 463–474.

Yokota, T., Miyagishi, M., Hino, T., *et al.* (2004). siRNA-based inhibition specific for mutant SOD1 with single nucleotide alternation in familial ALS, compared with ribozyme and DNA enzyme. Biochem. Biophys. Res. Commun. 314, 283–291.

Yokota, T., Sasaguri, H., Saito, Y., *et al.* (2007). Increase of disease duration of amyotrophic lateral sclerosis in a mouse model by transgenic small interfering RNA. Arch. Neurol. 64, 145–146.

Address correspondence to:
Dr. Takanori Yokota
Department of Neurology and Neurological Science
Graduate School, Tokyo Medical and Dental University
1-5-45, Yushima, Bunkyo-ku
Tokyo 113-8519
Japan

E-mail: tak-yokota.nuro@tmd.ac.jp

Received for publication February 11, 2012;
accepted after revision April 5, 2012.

Published online: April 6, 2012.

EXPERT OPINION

1. Introduction
2. Intravenous administration
3. Intracerebroventricular administration
4. Intranasal administration
5. Conclusion
6. Expert opinion

Short interfering RNA and the central nervous system: development of nonviral delivery systems

Kazutaka Nishina, Hidehiro Mizusawa & Takanori Yokota†
Tokyo Medical and Dental University, Graduate School, Department of Neurology and Neurological Science, Tokyo, Japan

The development of gene silencing therapies for neurological diseases has placed great importance on the delivery of short interfering RNA (siRNA) to the central nervous system (CNS). However, delivery of siRNA to neurons, glia and brain capillary endothelial cells (BCECs) has not been well established. This editorial describes different approaches that are being used to efficiently deliver siRNA to the CNS via intravenous, intracerebroventricular, or intranasal administration.

Keywords: central nervous system, intracerebroventricular administration, intranasal administration, intravenous administration, siRNA delivery

Expert Opin. Drug Deliv. (2013) 10(3):289-292

1. Introduction

Because no disease-modifying therapies are currently available to treat neurodegenerative diseases, such as Alzheimer's disease, Parkinson's disease, Huntington's disease and amyotrophic lateral sclerosis, silencing the causative gene using short interfering RNA (siRNA) is a promising method for treating these diseases. However, it is technically challenging to deliver siRNA to the central nervous system (CNS) because of the blood–brain barrier (BBB). The BBB is composed mainly of brain capillary endothelial cells (BCECs), pericytes and astrocyte foot processes. The BBB is both a physical barrier, resulting from the presence of endothelial tight junctions, and a transport barrier, resulting from the presence of selective membrane transporters and vesicular trafficking via BCECs. To cross the BBB, moieties must have a molecular weight of < 500 Da and be lipophilic [1]; siRNAs, however, have a molecular weight of > 14,000 Da and are hydrophilic. Improved delivery systems are therefore necessary to achieve effective gene silencing therapy in the CNS. Recently, several methods of delivering siRNAs to the CNS were developed. These methods include the use of hydrodynamic injection technique, conjugation of the siRNA to a lipid or peptide and the use of nanoparticles. The siRNAs were then administered through the intravenous (i.v.), intracerebroventricular (ICV), or intranasal (IN) routes. This editorial focuses on recent progress of administration to the CNS (**Table 1**).

2. Intravenous administration

A few reports have successfully delivered siRNA into the brain across the BBB [2-5]. At first, there are few reports using liposomes conjugated with peptidomimetic monoclonal antibody that bind to specific endogenous receptors (i.e., insulin and transferrin receptors) located on both the BBB and the brain cellular membranes [2].

informa
healthcare

10.1517/17425247.2013.748746 © 2013 Informa UK, Ltd. ISSN 1742-5247, e-ISSN 1744-7593

Table 1. Advantages and disadvantages of each administration route.

	Advantages	Disadvantages
i.v.	Be able to target whole brain including BBB	Difficult to pass through the BBB
ICV	Highly effective	Highly invasive
IN	Easiest and safest route of administration	Insufficient effect

Recent reports used the same short peptide derived from rabies viral glycoprotein (RVG) [3-5]. RVG interacts specifically with the nicotinic acetylcholine receptor (AChR) on neuronal cells to enable viral entry into the cells [3]. The nine-arginine-conjugated RVG peptide (RVG-9R) binds to negatively charged siRNA and can deliver siRNA to neural cells after i.v. administration [3]. This method has been used to specifically deliver siRNA to CNS cells, where it successfully inhibited the target endogenous gene [3]. The i.v. administration of RVG-9R was also used to target delivery of the siRNA to macrophages and microglial cells in the CNS [4]. Recently, i.v. administrated RVG-fused exosomes, which are endogenous nanovesicles that can transport materials including miRNA, were used in delivering siRNA specifically to neurons, microglia and oligodendrocytes in the brain, where it reduced the expression of an endogenous target gene [5]. Using siRNA-RVG exosome, no significant elevations of cytokines including IL-6, TNF-α and IFN-α were registered in contrast to siRNA-RVG-9R, which potently stimulated IL-6 secretion [5]. The mechanism by which RVG transverses the BBB is still not clear, but using RVG is a promising method for delivering siRNA across the BBB to the brain after i.v. administration.

Another drug delivery system to the neuron using i.v. administration, MRI-guided focused ultrasound (MRIgFUS), combined with intravascular delivery of microbubble contrast agent, was reported [6]. MRIgFUS was noninvasive delivery system of cholesterol-conjugated siRNA to CNS and was used to locally and transiently disrupt the BBB [6].

The BCECs are no longer regarded as an inert vascular lining that is injured and morphologically changed during the infarction, but are now understood to actively play many important roles in the pathophysiological mechanisms of ischemia, inflammation and transport across the BBB. Thus, gene silencing therapy in the BBB is being considered for the treatment of major neurological diseases, such as brain ischemia, multiple sclerosis and Alzheimer's disease. We first reported the delivery of siRNA into BCECs using a hydrodynamic injection technique [7]. However, hydrodynamic injection cannot be applied clinically because of the volume overload and extremely high hydrostatic pressure involved. Next, we reported the efficient delivery of siRNA into BCECs using an endogenous lipoprotein [8]. We chose to conjugate cholesterol to the siRNA for incorporation into extracted endogenous high-density lipoproteins (HDL), because cholesterol can be endocytosed via HDL receptors expressed in BCECs, but cannot enter the brain. Cholesterol-conjugated siRNA was successfully delivered into BCECs by receptor-mediated uptake and suppressed an endogenous gene in BCECs.

3. Intracerebroventricular administration

ICV administration can be used to bypass the BBB and other mechanisms that limit drug distribution into the brain [9]. Gene silencing using ICV administration of siRNA has been reported [10-12]. The ICV infusion of naked siRNA into the third ventricle of the mouse brain suppressed a target gene at a dose of 3 μmol [10], but another study showed that naked siRNA does not reach brain cells as well as naked antisense oligonucleotide after ICV administration [11]. To increase the stability and efficiency of siRNA, several chemical modifications ('Accell siRNA') have been introduced into siRNA nucleotides. Although its mechanism of delivery is unknown, chemically modified siRNA reduced expression of target genes in neurons, but not glia, after ICV administration [12]. These results suggest that chemical modification is necessary to deliver siRNA to the CNS even when using ICV administration.

We reported efficient siRNA delivery by ICV administration when using lipoprotein as an *in vivo* carrier for the siRNA [13]. We used α-tocopherol-conjugated siRNA to bind serum HDL, and we achieved dramatic improvement in siRNA delivery to neurons. In brain, α-tocopherol is incorporated into HDL-like particles that are synthesized in astrocytes and transferred to neurons and glial cells. Serum HDL and HDL-like particles have similar particle size and density and both use apolipoprotein E as a ligand for receptors. The dose of unconjugated siRNA needed for target suppression was as much as 3 μmol [9], whereas we found that only 3 nmol of α-tocopherol-conjugated siRNA with HDL could inhibit a target gene to a comparable degree [13].

Recently, the study showed chemically modified single-stranded siRNAs (ss-siRNAs) dramatically improve both potency and activity to treat model mouse of Huntington's disease by ICV administration [14]. The ss-siRNAs activity required chemical modifications including phosphorothioate linkages, 2′-methoxyribose, 2′-fluororibose, 2′-methoxyethyl-ribose, and 5-(*E*)-vinylphosphonate. The ss-siRNAs do not require special formulations to distribute to peripheral tissues, and it is very useful to clinical application.

4. Intranasal administration

IN administration is a noninvasive method of drug delivery that may also bypass the BBB to allow therapeutic substances, including siRNA, to cross to the CNS. The advantage of this method is the rapid onset of effects without injection. The

disadvantage of this route is that the limited absorption across the nasal epithelium has restricted its application to particularly potent substances [15].

One recent study examined the delivery of the chemically modified siRNA from the nasal cavity to the olfactory bulbs via the olfactory nerve pathway [16]. The chemically modified siRNA was delivered to the olfactory bulbs via the olfactory nerve but was not distributed to other regions of the brain [16]. Other studies of IN administration of siRNA using dendrimers [17,18] showed more efficient delivery of siRNA to additional brain regions, including the hypothalamus, amygdala, cerebral cortex and striatum [17]. IN administration of siRNA using e-PAM-R, a biodegradable poly(amidoamine) dendrimer, as a carrier reduced expression of the target gene *HMGB1* in the prefrontal cortex and striatum, and also suppressed infarct volume in the postischemic rat brain [17]. Another study that used poly (amidoamine) G7 dendrimers complexed with ^{32}P-labeled siRNA achieved higher brain radioactivity than that achieved by i.v. injection of dendriplexes or IN administration of naked siRNA [18]. These results indicate that the IN delivery of siRNAs complexed with dendrimers may be an efficient method of gene suppression therapy in the restricted area of the CNS.

5. Conclusion

Gene suppression using siRNA is a promising approach for treating neurodegenerative diseases. Several methods have shown efficacy in animal models, but further increase in the efficiency of delivery is needed.

6. Expert opinion

The use of siRNA as therapy for CNS disorders is currently under investigation, but getting siRNAs to cross the BBB and to be sufficiently available in the CNS upon systemic administration remains difficult. Each delivery route, i.v., ICV or IN, has advantages and disadvantages. The i.v. method is the most common administration route clinically, but it is still a big challenge to get the large, polar siRNA molecules to pass through the BBB. The ICV method more effectively suppresses target genes than the other routes, but it is invasive. The IN method is the easiest and safest route of administration, and it affords an opportunity for repeated self-administration, but its silencing effect is still weak.

In conclusion, these novel protocols we described are likely to be useful not only in experimental investigations but also in the clinical application of siRNA in the treatment of CNS disorders. Another useful chemical modification, conjugation of usable molecule, or using practical nanoparticle will be needed in order for siRNA to be used clinically in the CNS. Although further developments of these items are required, siRNA delivery strategies to the CNS are being used more widely, and we think that these methods should make treating CNS disorders possible.

Declaration of interest

This study was supported by grants from the National Institute of Biomedical Innovation, Japan (to T Yokota) and the Ministry of Health, Labor and Welfare, Japan (to T Yokota and H Mizusawa). The authors state no conflict of interest and have received no payment in preparation of this manuscript.

Bibliography

Papers of special note have been highlighted as either of interest (•) or of considerable interest (••) to readers.

1. Barchet TM, Amiji MM. Challenges and opportunities in CNS delivery of therapeutics for neurodegenerative diseases. Expert Opin Drug Deliv 2009;6(3):211-25
2. Boado RJ. Blood–brain barrier transport of non-viral gene and RNAi therapeutics. Pharm Res 2007;24(9):1772-87
3. Kumar P, Wu H, McBride JL, et al. Transvascular delivery of small interfering RNA to the central nervous system. Nature 2007;448(7149):39-43

•• **The first paper reporting transvascular delivery of siRNA to the CNS.**

4. Kim SS, Ye C, Kumar P, et al. Targeted delivery of siRNA to macrophages for anti-inflammatory treatment. Mol Ther 2010;18(5):993-1001
5. Alvarez-Erviti L, Seow Y, Yin H, et al. Delivery of siRNA to the mouse brain by systemic injection of targeted exosomes. Nat Biotechnol 2011;29(4):341-5

• **Use of RVG-fused exosomes to deliver siRNA across the BBB.**

6. Burgess A, Huang Y, Querbes W, et al. Focused ultrasound for targeted delivery of siRNA and efficient knockdown of Htt expression. J Control Release 2012;163(2):125-9
7. Hino T, Yokota T, Ito S, et al. In vivo delivery of small interfering RNA targeting brain capillary endothelial cells. Biochem Biophys Res Commun 2006;340(1):263-7
8. Kuwahara H, Nishina K, Yoshida K, et al. Efficient in vivo delivery of siRNA into brain capillary endothelial cells along with endogenous lipoprotein. Mol Ther 2011;19(12):2213-21

•• **The first report of siRNA delivery into BCECs using cholesterol-conjugated siRNA considerable clinical usage.**

9. Cook AM, Mieure KD, Owen RD, et al. Intracerebroventricular administration of drugs. Pharmacotherapy 2009;29(7):832-45
10. Thakker DR, Natt F, Hüsken D, et al. Neurochemical and behavioral consequences of widespread gene knockdown in the adult mouse brain by using nonviral RNA interference. Proc Natl Acad Sci USA 2004;101(49):17270-5

• **The first report of efficient ICV administration of siRNA.**

11. Senn C, Hangartner C, Moes S, et al. Central administration of small interfering RNAs in rats: a comparison with antisense oligonucleotides. Eur J Pharmacol 2005;522(1-3):30-7
12. Nakajima H, Kubo T, Semi Y, et al. A rapid, neuron-selective, in vivo knockdown following a single intracerebroventricular injection of a novel chemically modified siRNA in the adult rat brain. J Biotechnol 2012;157(2):326-33
13. Uno Y, Piao W, Miyata K, et al. High-density lipoprotein facilitates in vivo delivery of alpha-tocopherol-conjugated short-interfering RNA to the brain. Hum Gene Ther 2011;22(6):711-19

•• **ICV administration of α-tocopherol-conjugated siRNA is a highly efficient method of siRNA delivery.**

14. Yu D, Pendergraff H, Liu J, et al. Single-Stranded RNAs use RNAi to potently and allele-selectively inhibit mutant Huntingtin expression. Cell 2012;150(5):895-908

•• **The first report of efficient ICV administration of single-stranded siRNA.**

15. Lochhead JJ, Thorne RG. Intranasal delivery of biologics to the central nervous system. Adv Drug Deliv Rev 2012;64(7):614-28
16. Renner DB, Frey WH II, Hanson LR. Intranasal delivery of siRNA to the olfactory bulbs of mice via the olfactory nerve pathway. Neurosci Lett 2012;513(2):193-7
17. Kim ID, Shin JH, Kim SW, et al. Intranasal delivery of HMGB1 siRNA confers target gene knockdown and robust neuroprotection in the postischemic brain. Mol Ther 2012;20(4):829-39

•• **IN administration of siRNA dendriplexes is also an efficient siRNA delivery method.**

18. Perez AP, Mundiña-Weilenmann C, Romero EL, et al. Increased brain radioactivity by intranasal ^{32}P-labeled siRNA dendriplexes within in situ-forming mucoadhesive gels. Int J Nanomedicine 2012;7:1373-85

Affiliation

Kazutaka Nishina[1] MD PhD,
Hidehiro Mizusawa[2] MD PhD &
Takanori Yokota[†2] MD PhD
[†]Author for correspondence
[1]Medical Fellow,
Tokyo Medical and Dental University,
Graduate School,
Department of Neurology and Neurological Science,
1-5-45, Yushima, Bunkyo-ku,
Tokyo 113-8519, Japan
[2]Professor,
Tokyo Medical and Dental University,
Graduate School,
Department of Neurology and Neurological Science,
1-5-45, Yushima, Bunkyo-ku,
Tokyo 113-8519, Japan
Tel: +81 3 5803 5234;
Fax: +81 3 5803 0169;
E-mail: tak-yokota.nuro@tmd.ac.jp

siRNA conjugate

DOI: 10.1002/anie.200((will be filled in by the editorial staff))

Acidic pH-Responsive siRNA Conjugate for Reversible Carrier Stability and Accelerated Endosomal Escape without IFNα-Associated Immune Response **

Hiroyasu Takemoto, Kanjiro Miyata, Shota Hattori, Takehiko Ishii, Tomoya Suma, Satoshi Uchida, Nobuhiro Nishiyama and Kazunori Kataoka**

((Dedication----optional))

Small interfering RNA (siRNA) has garnered much interest as a potential drug because of its strong gene silencing activity [1]. Toward the success in siRNA therapeutics, many strategies have been developed for efficient siRNA delivery into the cytosol of target cells [2]. Among them, siRNA conjugates have arisen as one of the promising strategies in siRNA delivery, as siRNA can be readily conjugated to a functional molecule to acquire the ability of "programmed transfer" to the target sites [3]. Indeed, several ligand molecules, such as lactose and RGD peptide, were conjugated with siRNA for the site (or cell)-specific delivery [3]. Furthermore, multimolecular siRNA conjugates enable stable polyion complex (PIC) formation because of the increased electrostatic interactions with polycations, leading to facilitated cellular uptake through the charge neutralization of siRNA and also the protection of siRNA from enzymatic degradations [4]. However, those siRNA conjugates potentially stimulate immune responses through the activation of toll-like receptor 3 and/or protein kinase R [4, 5], and thus they are desired to disintegrate into monomeric siRNAs (mono-siRNAs) in the cell for reduced immune responses [4]. Meanwhile, considering that macromolecular drugs, including siRNA and its conjugates, would be uptaken by cells through endocytosis and then delivered to the late endosome toward lysosomal degradation, siRNA needs to escape from the endosome into the cytosol for efficient gene silencing [6]. Therefore, design of a smart siRNA conjugate for programmed endosomal escape and release of mono-siRNA is a great challenge for successful siRNA delivery.

In this study, we developed a smart siRNA conjugate to fulfill the multifunctionality desired for enhanced siRNA delivery with reduced immunogenicity, i.e., reversible PIC stability, endosomal escapability, and mono-siRNA releasability, based on single chemistry. It is known that maleic acid amide (MAA) is relatively stable at extracellular neutral pH, while rapidly hydrolyzed at endosomal acidic pH [7]. Thus, we developed this MAA chemistry as an acid-labile anionic moiety for linking siRNA to an endosome-disrupting polycation and concurrently converting the cationic sites to a biologically inert anionic derivative [8]. In design, the MAA-based conjugate is expected to improve the PIC stability through increased electrostatic interaction, while degrading the MAA moieties in the endosome for triggering three actions, i) complex destabilization through unbalanced charges within PICs, ii) endosome disruption with the regenerated parent polycation, and iii)

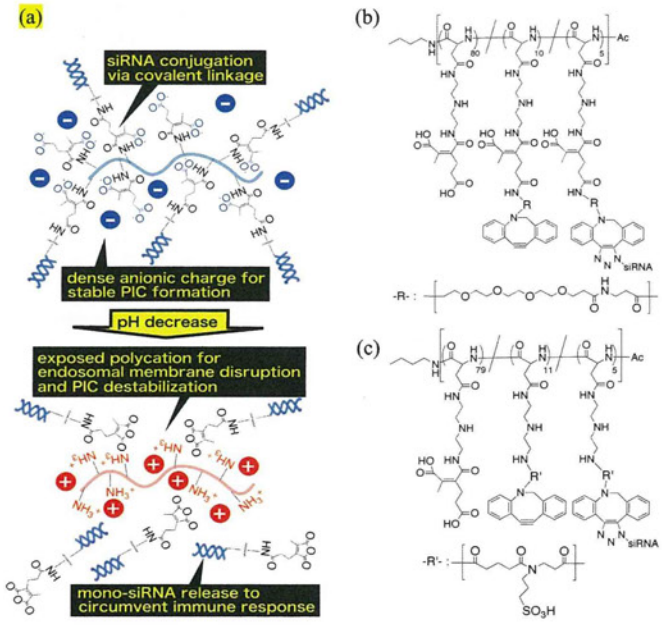

Figure 1. (a) Schematic illustration of REC with the multifunctionality toward endosomal escape and release of mono-siRNA. (b) Chemical structure of REC. (c) Chemical structure of uREC. PAsp derivative in this study has the mixed sequence of α and β isomers. Only α isomers are depicted in the Figures 1b and 1c for the simplicity.

[*] H. Takemoto and Dr. K. Kataoka
Department of Materials Engineering
The University of Tokyo
Hongo 7-3-1, Bunkyo-ku, Tokyo 113-8656 (Japan)
Fax: +81-3-5841-7139
E-mail: kataoka@bmw.t.u-tokyo.ac.jp
Homepage: http://www.bmw.t.u-tokyo.ac.jp/

S. Hattori, Dr. T. Ishii and T. Suma
Department of Bioengineering, The University of Tokyo
Hongo 7-3-1, Bunkyo-ku, Tokyo 113-8656 (Japan)

Dr. K. Miyata and S. Uchida
Division of Clinical Biotechnology, Center for Disease Biology and Integrative Medicine, The University of Tokyo
Hongo 7-3-1, Bunkyo-ku, Tokyo 113-8656 (Japan)
Fax: +81-3-5841-7139
E-mail: miyata@bmw.t.u-tokyo.ac.jp

Dr. N. Nishiyama
Polymer Chemistry Division, Chemical Resources Laboratory, Tokyo Institute of Technology, R1-11, 4259 Nagatsuta, Midori-ku, Yokohama 226-8503, Japan

[**] This research is supported by the Japan Society for the Promotion of Science (JSPS) through the "Funding Program for World-Leading Innovative R&D on Science and Technology (FIRST Program)," and Health and Labour Sciences Research Grants Research on Medical Device Development, Ministry of Health, Labour and Welfare. H. Takemoto thanks the Research Fellowships of the Japan Society for the Promotion of Science for Young Scientists (JSPS).

Supporting information for this article is available on the WWW under http://www.angewandte.org or from the author.

mono-siRNA release via the MAA cleavage, as illustrated in Figure 1a. Figure 1b shows the chemical structure of siRNA-releasable/endosome-disrupting conjugate (REC), in which several siRNA molecules are grafted into the endosome-disrupting polymer side chains via MAA linkage. The parent polycation is a polyaspartamide derivative with two repeating units of aminoethylene in each side chain (termed PAsp(DET)), which destabilizes the endosomal membrane integrity with the cationic diprotonated side chains to accelerate endosomal escape of the payload [9].

A precursor polyanion was synthesized from PAsp(DET) to have dibenzyl cyclooctyne (DBCO) group via MAA linkage as a conjugation site for siRNA. Then, an azide-modified siRNA (azide-siRNA) was reacted with the DBCO group in the polyanion side chains (Supporting Scheme 5). It should be noted that more than 95% of azide-siRNAs were conjugated to the polymer backbone utilizing a unique technique of "freeze-thawing treatment" for generation of highly-concentrated reactant phase [10], as determined by size exclusion chromatography (Supporting Figure 5). As a result, ~30% of DBCO groups in the polymer side chains reacted with azide-siRNA, i.e., ~5 siRNAs contained in the conjugate (Figure 1b). To investigate the effect of MAA linkage on the siRNA-releasability, another siRNA conjugate, where the DBCO group was directly conjugated to primary amines in PAsp(DET) without MAA linkage, was also synthesized as an siRNA-unreleasable but endosome-disrupting control (uREC) (Figure 1c). The obtained siRNA conjugates were analyzed for their pH-sensitivity by polyacrylamide gel electrophoresis (PAGE) analysis (Figure 2a). The retarded bands in siRNA conjugates, compared to mono-siRNA, indicate that both siRNA conjugates had significantly higher molecular weight than mono-siRNA. A 1 h incubation of REC at pH 5.0 resulted in the band appearance at the same position as mono-siRNA, whereas such band was not observed at pH 7.4, indicating that mono-siRNA release was triggered selectively at the acidic pH. In contrast, the band corresponding to mono-siRNA was not observed for uREC after a 1 h incubation at both pHs of 5.0 and

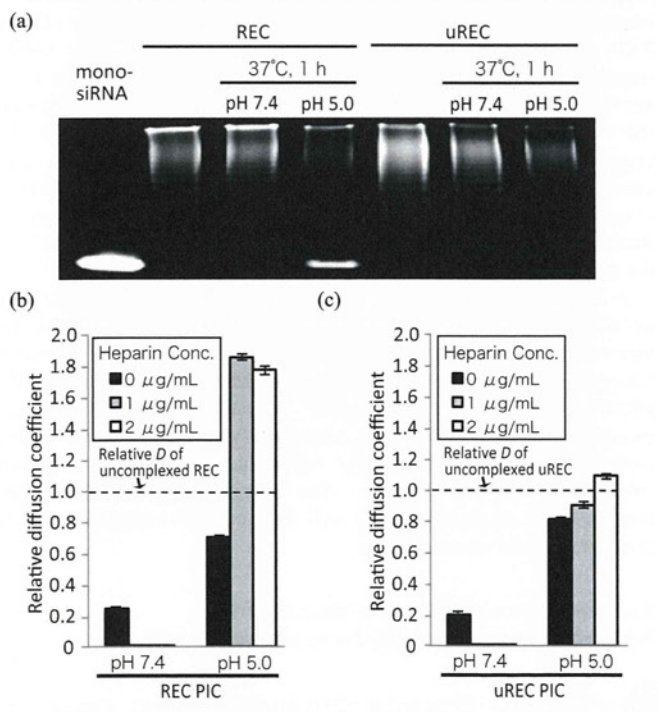

Figure 2. (a) PAGE analysis of REC and uREC before and after a 1 h incubation at 37 °C and at pH 7.4 or pH 5.0. (b, c) Relative *D*s of siRNA conjugate PICs after a 30 min incubation at 37 °C with various heparin concentrations at pH 7.4 or pH 5.0. Relative *D*s are calculated by normalization of *D*s to that of uncomplexed siRNA conjugates; REC PIC (b) and uREC PIC (c). Results were shown as mean and standard deviation obtained from 10 measurements.

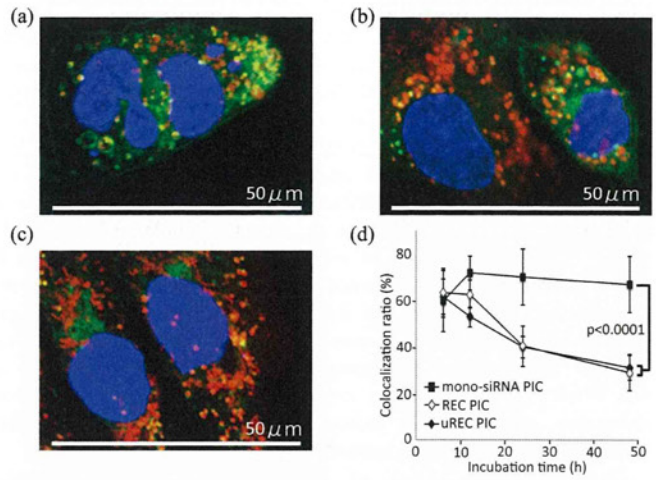

Figure 3. (a-c) CLSM images 48 h after treatment of SKOV3-Luc cells with mono-siRNA PIC (a), REC PIC (b), and uREC PIC (c). Red: Cy3-siRNA, green: late endosome/lysosome (LysoSensor Green), blue: nucleus (Hoechst 33342). Yellow pixel indicates colocalization between red pixel and green pixel. (d) Time-dependent change in the colocalization ratio between Cy3-siRNA and late endosome/lysosome. The colocalization ratio was shown as mean and standard deviation obtained from 10 cells. P value was calculated according to Student's t test.

7.4, indicating the essential role of MAA linkage for mono-siRNA release from REC.

Next, siRNA conjugates were mixed with a polycation PAsp(DET) to form PICs at N/P 10 (residual molar ratio of amines of PAsp(DET) to phosphates of siRNA) for their facilitated cellular uptake. PIC formation with siRNA conjugates as well as mono-siRNA was confirmed by fluorescence correlation spectroscopy (FCS) using Cy3-labeled siRNA (Cy3-siRNA) and its conjugates (Supporting Table 2) as well as agarose gel electrophoresis (Supporting Figure 6). The diffusion coefficients (*D*s) in 10 mM HEPES buffer (pH 7.4) were determined to be 66.2 μm^2/sec for mono-siRNA PIC and 2.9 μm^2/sec for both siRNA conjugate PICs. These values were significantly smaller than those of the uncomplexed controls, i.e., mono-siRNA (94.5 μm^2/sec) and siRNA conjugates (15.5 μm^2/sec for REC and 18.8 μm^2/sec for uREC). Considering that *D* of nanoparticles is inversely correlated with their size [11], the smaller *D*s in the presence of polycation indicate successful PIC formation with the siRNA conjugates as well as mono-siRNA in the aqueous condition (siRNA concentration: 100 nM). The substantially smaller *D*s of the conjugate PICs, compared to the mono-siRNA PIC, indicate a larger association number of siRNA in the conjugate PICs presumably due to increased anionic charges in the conjugate. Then, the acidic pH-sensitivity in the PIC was further evaluated by FCS after a 30 min incubation of PICs at 37 °C in 10 mM HEPES (pH 7.4) and 10 mM MES (pH 5.0) containing heparin. Heparin is a major component of extracellular matrices on cellular surface and probably serves as a strong polyanionic counterpart to induce PIC dissociation [12]. The obtained *D*s of each sample were normalized to that of the corresponding uncomplexed siRNA control, i.e., uncomplexed REC for REC PIC, uncomplexed uREC for uREC PIC, and uncomplexed mono-siRNA for mono-siRNA PIC (Figure 2b, 2c, and Supporting Figure 7, respectively). After incubation with heparin, a relative *D* of mono-siRNA PICs progressively increased with the increase in heparin concentration similarly at both pHs of 7.4 and 5.0, indicating that mono-siRNA PICs gradually dissociated with the increased counter polyanion regardless of the environmental pHs (Supporting Figure 7). In contrast, relative *D*s of REC and uREC PICs decreased after incubation with heparin at pH 7.4, suggesting

that siRNA (or its conjugate) is stably encapsulated in PICs even after binding of heparin onto PIC surface. Notably, the incubation of REC and uREC PICs at pH 5.0 dramatically increased their relative *D*s, and further, the increase in the relative *D*s was facilitated in the presence of heparin, indicating the acidic pH-responsive destabilization of the siRNA conjugate PICs (Figure 2b and 2c). Considering the fact that the MAA linkage contained in both siRNA conjugates can degrade at pH 5.0 to generate the polycations in PIC, the destabilization of siRNA conjugate PICs at pH 5.0 is presumably due to the electrostatic repulsion between the generated polycations and the originally incorporated polycations in PIC. In addition, the increased relative *D*s of REC PICs in the presence of heparin, beyond that of uncomplexed REC, strongly suggest the mono-siRNA release triggered by the cleavage of MAA linkage. These results demonstrate that the acidic pH-sensitivity of the MAA-based conjugates can be maintained even after PIC formation, and also they provide siRNA PICs with a reversible stability in response to the intracellular environment.

Delivery functionalities of REC PICs, i.e., cellular uptake efficiency and intracellular trafficking profile, were evaluated with cultured human ovarian cancer cells stably expressing luciferase (SKOV3-Luc). Cellular uptake of siRNA was estimated using Cy3-siRNA with a fluorescence microscopy (Supporting Figure 8). REC and uREC PICs (N/P 10) allowed 30% increase in Cy3 fluorescence from cells, compared to mono-siRNA PICs (N/P 10, $p < 0.005$), indicating that the conjugate formulation significantly enhanced the cellular uptake of siRNA probably due to the higher stability, as suggested by the FCS result at pH 7.4 (Figure 2b, 2c, and Supporting Figure 7). Next, confocal laser scanning microscopic (CLSM) observation was performed to examine subcellular distribution of siRNA PICs (N/P 10), especially focusing on the colocalization of siRNA with the late endosome/lysosome as an indicator for endosomal entrapment (Figure 3a-c) [13]. In the cells treated with mono-siRNA PICs, the colocalization (yellow) ratio of Cy3-siRNA (red) with a late endosome/lysosome marker LysoSensor Green (green) was increased up to 70 % for the initial 12 h and then kept constant for subsequent 36 h (Figure 3d). In contrast, the cells treated with REC and uREC PICs showed that the colocalization ratio was progressively decreased over incubation period and reached ~30% after a 48 h incubation. The significantly lower colocalization ratios (or less endosomal entrapment) of REC/uREC PICs strongly suggest more efficient endosomal escape of siRNA, compared to mono-siRNA PICs (Figure 3d). This enhanced endosomal escape with REC and uREC is consistent with the endosome-disrupting functionality of the backbone polymer, which should be converted to the parent polycation PAsp(DET) in the acidic late endosome/lysosome for the membrane disruption, as suggested by a membrane disruption assay at pH 7.4 and 5.0 (Supporting Figure 9) [8, 9].

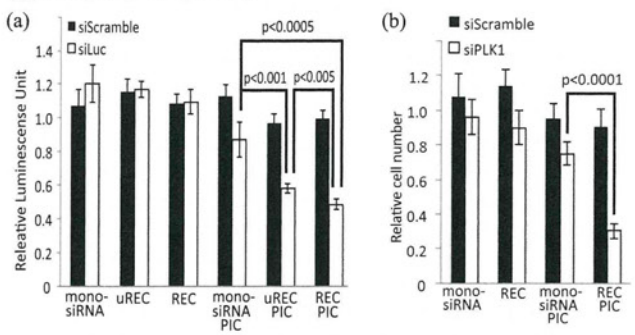

Figure 4. (a) Luciferase gene expression in cultured SKOV3-Luc cells after PIC treatment at 100 nM Luc siRNA (siLuc) or scramble siRNA (siScramble) for 48 h. (b) Cell viability in cultured A549 cells after PIC treatment at 100 nM PLK1 siRNA (siPLK1) or siScramble for 72 h. In both figures, results were shown as mean and standard deviation obtained from 6 samples. P value was calculated according to Student's t test.

Next, gene silencing ability of REC PICs was compared with mono-siRNA and uREC PICs by luciferase assay with cultured SKOV3-Luc cells (Figure 4a). Obviously, REC and uREC PICs achieved more efficient sequence-specific gene silencing in the cells than mono-siRNA PICs, presumably due to the enhanced endosomal escape of siRNA conjugate PICs (Figure 3) as well as facilitated cellular uptake of siRNA (Supporting Figure 8). Interestingly, REC PICs induced significantly stronger gene silencing than uREC PICs ($p < 0.005$), demonstrating the positive effect of siRNA releasability via MAA linkage on siRNA delivery functionality. Mono-siRNA releasates from REC might be more readily associated with the gene silencing pathway due to compromised steric hindrance, compared to the conjugated structure. Also, no cytotoxicity was observed for all the tested PIC formulations under the same condition as the gene silencing assay (Supporting Figure 10). Note that significantly stronger luciferase gene silencing of REC PICs was also confirmed in comparison with mono-siRNA PICs prepared with PAsp(DET)/PAsp(DET-CDM) (a non-covalent control) and a commercially available reagent ExGen500 (linear polyethylenimine) (Supporting Figure 11), demonstrating the advantage of REC formulation, including covalent conjugation between siRNA and the backbone polymer. The effect of the siRNA-releasability of REC was further examined from the standpoint of immune responses; IFNα response was determined as an indicator of immune response by enzyme-linked immunosorbent assay (ELISA). REC, uREC, and their PICs did not induce a detectable level of IFNα production for SKOV3-Luc cells (< 10 pg/mL, data not shown). Thus, the similar ELISA experiment was further challenged for murine macrophage cells (Raw264.7), which are known to be highly sensitive to immunogen [14]. As a result, REC PICs induced a significantly lower level of IFNα production (24.3 ± 3.5 pg/mL) compared to uREC PICs (60.8 ± 12.9 pg/mL, $p < 0.005$), indicating that the siRNA-releasability based on MAA linkage successfully decreased the immune response for siRNA conjugates. Note that uncomplexed REC and uREC without polycation did not induce a detectable level of IFNα production, suggesting that they should not stimulate IFNα response at least on the cellular surface. Finally, the utility of REC PICs was verified for other cell lines, using a therapeutic siRNA targeting polo-like kinase 1 (PLK1). PLK1 is known to be a cell cycle regulator, and thus its silencing can arrest the cell cycle toward the apoptosis [15]. REC PICs with PLK1 siRNA (N/P 20) sequence-specifically suppressed the growth of human lung carcinoma cells (A549) and human hepatocarcinoma cells (Huh-7) (Figure 4b and Supporting Figure 12, respectively), demonstrating a strong potential of the REC formulation bearing the MAA linkage for siRNA-based cancer therapy.

In summary, an acidic pH-responsive siRNA conjugate was developed for enhanced siRNA delivery with reduced immunogenicity. Single chemistry based on MAA linkage successfully provided the multifunctionality required for successful siRNA delivery, i.e., reversible carrier stability, endosomal escapability, and mono-siRNA releasability. Ultimately, the siRNA conjugate sequence-specifically achieved the significant growth inhibition of cancerous cells. The programmed siRNA delivery based on the smart conjugate will be further investigated for the success in siRNA therapeutics.

Received: ((will be filled in by the editorial staff))
Published online on ((will be filled in by the editorial staff))

Keywords: siRNA · Drug design · Drug delivery · Polymers · Conjugation

[1] a) S. M. Elbashir, J. Harborth, W. Lendeckel, A. Yalcin, K. Weber, T. Tuschl, *Nature* **2001**, 41, 494-498; b) J. C. Burnett, J. J. Rossi, *Chem. Biol.* **2012**, 19, 60-71.

[2] R. L. Kanasty, K. A. Whitehead, A. J. Vegas, D. G. Anderson, *Mol. Ther.* **2012**, 20, 513-524.

[3] a) D. B. Rozema, D. L. Lewis, D. H. Wakefield, S. C. Wong, J. J. Klein, P. L. Roesch, S. L. Bertin, T. W. Reppen, Q. Chu, A. V. Blokhin, J. E. Hagstrom, J. A. Wolf, *Proc. Natl. Acad. Sci. USA* **2007**, 104, 12982 – 12987; b) Y. Singh, P. Murat, E. Defrancq, *Chem. Soc. Rev.* **2010**, 39, 2054-2070; c) M. R. Alam, X. Ming, M. Fisher, J. G. Lackey, K. G. Rajeev, M. Manoharan, R. L. Juliano, *Bioconjugate Chem.* **2011**, 22, 1673-1681; d) S. K. Lee, A. Siefert, J. Beloor, T. M. Fahmy, P. Kumar, *Methods Enzymol.* **2012**, 502, 91-122.

[4] a) A.-L. B.-Bellemin, M.-E. Bonnet, G. Creusat, P. Erbacher, J.-P. Behr, *Proc. Natl. Acad. Sci. USA* **2007**, 104, 16050-16055; b)H. Mok, S. H. Lee, J. W. Park, T. G. Park, *Nat. Mat.* **2010**, 9, 272-278; c) H. Takemoto, A. Ishii, K. Miyata, M. Nakanishi, M. Oba, T. Ishii, Y. Yamasaki, N. Nishiyama, K. Kataoka, *Biomaterials* **2010**, 31, 8097-8105; d) C. A. Hong, S. H. Lee, J. S. Kim, J. W. Park, K. H. Bae, H. Mok, T. G.Park, H. Lee, *J. Am. Chem. Soc.* **2011**, 133, 13914-13917; e) S. J. Lee, M. S. Huh, S. Y. Lee, S. Min, S. Lee, H. Koo, J. U. Chu, K. E. Lee, H. Jeon, Y. Choi, K. Choi, Y. Byun, S. Y. Jeong, K. Park, K. Kim, I. C. Kwon, *Angew. Chem.* **2012**, 124, 7315–7319; *Angew. Chem. Int. Ed.* **2012**, 51, 7203–7207.

[5] A. Judge, I. MacLachlan, *Hum. Gene Ther.* **2008**, 19, 111-124

[6] a) C. Troiber, E. Wagner, *Bioconjugate Chem.* **2011**, 22, 1737-1752; b) J. Nguyen, F. C. Szoka, *Acc. Chem. Res.* **2012**, 45, 1153-1162.

[7] a) D. B. Rozema, K. Ekena, D. L. Lewis, A. G. Loomis, J. A. Wolff, *Bioconjugate Chem.* **2003**, 14, 51-57; b) S. Guo, Y. Huang, Q. Jiang, Y. Sun, L. Deng, Z. Liang, Q. Du, J. Xing, Y. Zhao, P. C. Wang, A. Dong, X.-J., Liang, *ACS Nano* **2010**, 4, 5505-5511.

[8] Y. Lee, K. Miyata, M. Oba, T. Ishii, S. Fukushima, M. Han, H. Koyama, N. Nishiyama, K. Kataoka, *Angew. Chem.* **2008**, 120, 5241–5244; *Angew. Chem. Int. Ed.* **2008**, 47, 5163–5166.

[9] K. Miyata, M. Oba, M. Nakanishi, S. Fukushima, Y. Yamasaki, H. Koyama, N. Nishiyama, K. Kataoka, *J. Am. Chem. Soc.* **2008**, 130, 16287-16294.

[10] H. Takemoto, K. Miyata, T. Ishii, S. Hattori, S. Osawa, N. Nishiyama, K. Kataoka, *Bioconjugate Chem.* **2012**, 23, 1503-1506.

[11] J. DeRouchey, C. Schmidt, G. F. Walker, C. Koch, C. Plank, E. Wagner, J. O. Radler, *Biomacromolecules* **2008**, 9, 724-732.

[12] a) M. J. Palte, R. T. Raines, *J. Am. Chem. Soc.* **2012**, 134, 6218-6223; b) M. Zheng, D. Librizzi, A. Kılıç, Y. Liu, H. Renz, O. M. Merkel, T. Kissel, *Biomaterials* **2012**, 33, 6551-6558.

[13] K. Whitehead, G. Sahay, G. Z. Li, K. T. Love, C. A. Alabi, M. Ma, C. Zurenko, W. Querbes, R. S. Langer, D. G. Anderson, *Mol. Ther.* **2011**, 19, 1688-1694.

[14] J. Turco, H. H. Winker, *Infect. Immun.* **1982**, 35, 783-791

[15] a) A. D. Judge, M. Robbins, I. Tavakoli, J. Levi, L. Hu, A. Fronda, E. Ambegia, K. McClintock, I. MacLachlan, *J. Clin. Invest.* **2009**, 119, 661-673; b) K. Strebhardt, *Nat. Rev. Drug Discov.* **2010**, 9, 643-660.

Entry for the Table of Contents (Please choose one layout)

Layout 1:

siRNA-conjugate

Hiroyasu Takemoto, Kanjiro Miyata, Shota Hattori, Takehiko Ishii, Tomoya Suma, Satoshi Uchida, Nobuhiro Nishiyama and Kazunori Kataoka* _____ **Page – Page**

Acidic pH-Responsive siRNA Conjugate for Accelerated Endosomal Escape and Reduced Immunogenicity

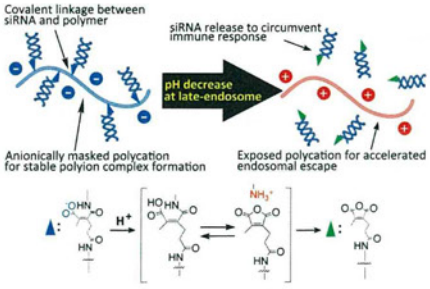

A smart siRNA conjugate was developed based on acid-labile maleic acid amide linkage for programmed transfer of siRNA from the endosome to the cytosol and concurrent siRNA release in the cell interior. Polyion complex with the conjugate allowed efficient cellular uptake and endosomal escape of siRNA as well as reversible stability in response to endosomal acidic pH. Ultimately, the complexed conjugate achieved the potent gene silencing in various cultured cancerous cells with negligible adverse side effects.

Bioorganic & Medicinal Chemistry 21 (2013) 1717–1723

Contents lists available at SciVerse ScienceDirect

Bioorganic & Medicinal Chemistry

journal homepage: www.elsevier.com/locate/bmc

Synthesis and properties of cationic oligopeptides with different side chain lengths that bind to RNA duplexes

Yusuke Maeda, Rintaro Iwata, Takeshi Wada *

Department of Medical Genome Sciences, Graduate School of Frontier Sciences, The University of Tokyo, Bioscience Building 702, Kashiwanoha, Kashiwa, Chiba 277-8562, Japan

ARTICLE INFO

Article history:
Received 4 January 2013
Revised 22 January 2013
Accepted 23 January 2013
Available online 1 February 2013

Keywords:
RNA-binding peptide
Cationic peptide
Artificial peptide
RNAi drug
DDS

ABSTRACT

A series of artificial peptides bearing cationic functional groups with different side chain lengths were designed, and their ability to increase the thermal stability of nucleic acid duplexes was investigated. The peptides with amino groups selectively increased the stability of RNA/RNA duplexes, and a relationship between the side chain length and the melting temperature (T_m) of the peptide–RNA complexes was observed. On the other hand, while peptides with guanidino groups exhibited a similar tendency with respect to the peptide structure and thermal stability of RNA/RNA duplexes, those with longer side chain lengths, such as L-2-amino-4-guanidinobutyric acid (Agb) or L-arginine (Arg) oligomers, stabilized both RNA/RNA and DNA/DNA duplexes, and those with shorter side chain lengths exhibited a higher ability to selectively stabilize RNA/RNA duplexes. In addition, peptides were designed with different levels of flexibility by introducing glycine (Gly) residues into the L-2-amino-3-guanidinopropionic acid (Agp) oligomers. It was found that insertion of Gly did not affect the thermal stability of the peptide–RNA complexes, but an alternate arrangement of Gly and Agp apparently decreased the thermal stability. Therefore, in the Agp oligomer, consecutive Agp sequences are essential for increasing the stability of RNA/RNA duplexes.

1. Introduction

In recent years, increased attention has been paid to the development of nucleic acid drugs. For example, antisense oligonucleotides and RNA interference drugs (RNAi drugs) are well known molecular tools for the regulation of gene expression, in which their mechanisms of action are based on sequence specific interactions.[1] The RNAi drugs act on the target mRNA in a sequence selective manner. Thus, RNAi drugs are attractive because of their high selectivity for the target and their shorter drug development time. Therefore, siRNAs have been widely studied for therapeutic applications; however, such RNA molecules are not sufficiently effective because of their low-membrane permeability and instability in cells. To stabilize oligonucleotides against metabolic degradation, a number of chemical modifications have been proposed,[2] and RNAi drugs generally consist of double stranded RNAs (dsRNAs) with chemical modifications. A proper modification of an RNA molecule increases its stability in cells and improves its pharmacokinetic properties.[3] Another strategy for stabilizing siRNA is the use of molecules that can non-covalently bind to RNA to protect it from attack by nucleases. For example, a fusion protein of the peptide transduction domain-dsRNA binding domain was shown to effectively transport RNAi drugs into primary cells.[4] In this case, the increased thermal stability of the dsRNAs also increased their stability in cells.[5] We are thus attempting to develop RNA/RNA duplex-binding molecules that are useful as drug delivery systems (DDSs) for siRNAs.

A wide variety of RNA-binding molecules have been reported, such as aminoglycosides[6] and RNA-binding proteins.[7] In paticular, chemically modified peptides bearing different methylene lengths in the arginine or lysine residues possess diverse affinities to RNAs.[8] In our previous study, α-(1 → 4)-linked-2,6-diamino-2,6-dideoxy-D-glucopyranose oligomers were synthesized, and their highly RNA-selective binding ability was demonstrated.[9] These results suggested that the geometry of the cationic groups, particularly the distance between the cationic groups, affects the affinity and selectivity of the oligomers for nucleic acid duplexes. Therefore, in this study, we designed a series of cationic oligopeptides to reveal the relationship between the geometry of the cationic groups and the affinity of the peptides for nucleic acids. In contrast to oligosaccharide derivatives, peptides can easily be synthesized, which is advantageous for obtaining a systematic series of molecules. They can also be readily connected with other functional groups such as transporter molecules.[10] Therefore, RNA duplex-binding peptides are useful tools for the development of drug delivery systems (DDSs) for RNAi drugs. The L-arginine (Arg) oligomers designed from the HIV Tat peptide are well known for their high-membrane permeability[11] and the Arg 15mer has been used as an RNAi transporter by forming a complex with RNA.[12]

* Corresponding author. Tel.: +81 4 7136 3611.
E-mail address: wada@k.u-tokyo.ac.jp (T. Wada).

0968-0896/$ - see front matter © 2013 Elsevier Ltd. All rights reserved.
http://dx.doi.org/10.1016/j.bmc.2013.01.053

However, the activity varies with the side chain length,[13] and thus a more detailed study of the relationship between the structure and activity is important for the development of effective carriers for RNAi drugs. Thus, to investigate the structural effects on binding ability, we designed and synthesized a number of cationic oligopeptides bearing different side chain lengths to control the distance between the cationic functional groups and peptides with different flexibility by incorporating glycine (Gly).

2. Results and discussion

2.1. Design of the peptides

A series of cationic oligopeptides was designed (Fig. 1). All peptides contained a unit of *N*-acetyl-L-tyrosine with two glycine residues at the N-terminus for UV detection and quantification. In this study, the 12mer of nucleic acid duplexes was used as a model to estimate the interaction with peptides bearing four or eight cationic groups because four pairs of phosphate groups are aligned on the inward portion of the major groove of the 12mer of A-type nucleic acid duplexes. First, to compare the effects of the distance between cationic groups, peptides with different side chain lengths were designed. Peptides were synthesized with amino groups (L-2,3-diaminopropionic acid (Dap), L-2,4-diaminobutyric acid (Dab), L-ornithine (Orn), and L-lysine (Lys)) and guanidino groups (L-2-amino-3-guanidinopropionic acid (Agp), L-2-amino-4-guanidinobutyric acid (Agb), and L-arginine (Arg)). In some molecules, several glycine units were also inserted into an Agp octamer to increase the flexibility of the peptides. Peptides with alternate arrangements were also designed to change the position and combination of the functional groups. These peptides were based on the Agp oligomer and other amino acids such as glycine (Gly), L-serine (Ser), and L-asparagine (Asn). Glycine was chosen because of its high flexibility. Ser and Asn were chosen because they are well known in RNA-binding proteins to form hydrogen bonds with the phosphate groups of RNA.[14]

On the basis of molecular mechanics calculations with a GB/SA water solvation model,[15] a cationic oligopeptide 8mer consisting of Dab can bind to the major groove of an A-type RNA/RNA duplex 12mer, in which all the protonated amino groups of the peptide form the hydrogen bonds to the phosphate anions of the duplex (Fig. 2). Therefore, the electrostatic interaction and hydrogen bonding would be important for the binding of cationic oligopeptides to RNA/RNA duplexes.

2.2. Melting temperature (T_m) analysis

The T_m values of the RNA duplexes were measured both in the absence and presence of an equal amount of peptides. All measurements were performed under-physiological conditions with 10 mM phosphate buffer containing 100 mM NaCl at pH 7.0. Figure 2 shows the melting temperature enhancements and Table 1 lists the T_m values for the self complementary RNA 12mer r(CGCGAAUUCGCG)$_2$ in the absence and presence of an equal amount of peptides with amino groups. In this study, the peptides were added into the solution of nucleic acid duplexes after annealing to avoid the aggregation of the peptides at high temperature. The T_m values were affected by the side chain length, with Dab_8 (**2**) showing the highest T_m value. Comparing the Dab_8 (**2**), Orn_8 (**3**), and Lys_8 (**4**), the T_m value increased as the side chain length

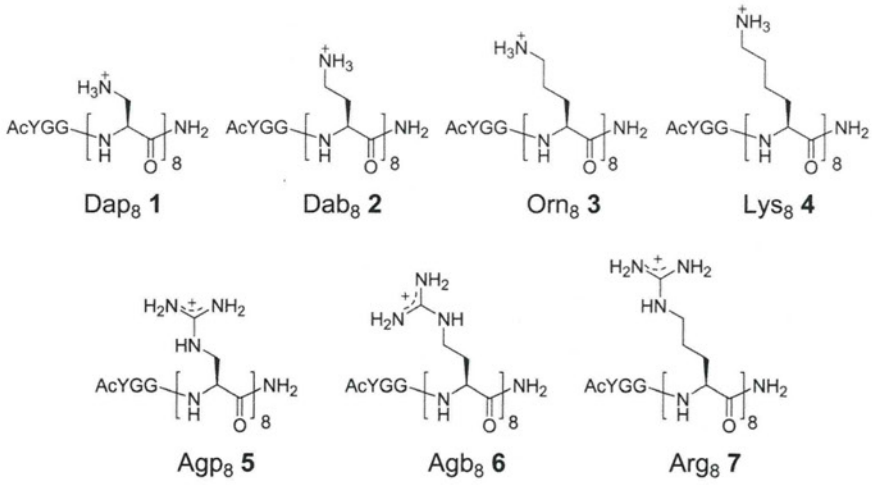

Peptides with amino groups

Dap_8	:	Ac-YGG-Dap_8-NH_2 **1**	
Dab_8	:	Ac-YGG-Dab_8-NH_2 **2**	
Orn_8	:	Ac-YGG-Orn_8-NH_2 **3**	
Lys_8	:	Ac-YGG-Lys_8-NH_2 **4**	

Peptides with guanidino groups

Agp_8	:	Ac-YGG-Agp_8-NH_2 **5**	
Agb_8	:	Ac-YGG-Agb_8-NH_2 **6**	
Arg_8	:	Ac-YGG-Arg_8-NH_2 **7**	

Peptides with flexible main chains

Agp_8G1	:	Ac-YGG-Agp_4-G-Agp_4-NH_2	**8**
Agp_8G2	:	Ac-YGG-Agp_3-G-Agp_2-G-Agp_3-NH_2	**9**
Agp_8G3	:	Ac-YGG-Agp_2-G-Agp_2-G-Agp_2-G-Agp_2-NH_2	**10**
Agp_8A2	:	Ac-YGG-Agp_3-A-Agp_2-A-Agp_3-NH_2	**11**
Agp_8P2	:	Ac-YGG-Agp_3-P-Agp_2-P-Agp_3-NH_2	**12**

Peptides with alternate arrangement

AgpG	:	Ac-YGG-$(Agp\text{-}G)_4$-NH_2	**13**
AgpS	:	Ac-YGG-$(Agp\text{-}S)_4$-NH_2	**14**
AgpN	:	Ac-YGG-$(Agp\text{-}N)_4$-NH_2	**15**

Figure 1. Structures and sequences of cationic peptides.

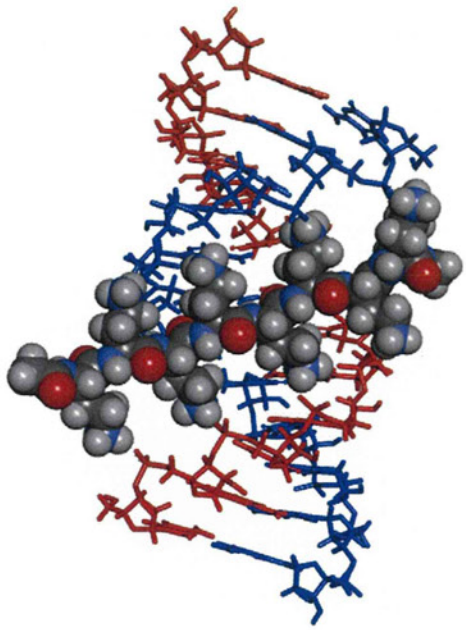

Figure 2. Molecular model of L-2,4-diaminobutylic acid (Dab) 8mer binding to A-type RNA–RNA duplex (12mer).

Table 1
Thermal melting points (T_m in °C) for oligonucleotide duplex (in the absence and presence of peptides with amino groups[a])[b]

Peptide	RNA/RNA	ΔT_m	DNA/DNA	ΔT_m
None	60.7		48.2	
Dap_8	60.2	−0.5	50.8	2.6
Dab_8	74.7	14.0	49.5	1.3
Orn_8	74.2	13.5	51.3	3.1
Lys_8	68.1	7.4	49.7	1.5

[a] Peptide concentration 4 μM.
[b] Buffer (10 mM phosphate buffere for pH 7.0), NaCl (100 mM), together with each oligonucleotide strand (4 μM). T_m values are reported at the means of duplicate measurements.

decreased. These results suggest that the distance between the amino groups in Dab_8 (**2**) fits to the distance of the opposing phosphate groups in the RNA duplexes. This tendency has been previously reported for cationic oligopeptides with D-amino acids.[6] On the other hand, Dap_8 (**1**) did not stabilize the RNA/RNA duplexes. This differing behavior may result because the distance of the amino groups in Dap_8 is too short to interact with the phosphate groups in the RNA/RNA duplexes. In fact, none of the peptides with amino groups increased the thermal stability of the DNA/DNA duplex d(CGCGAATTCGCG)$_2$ (Fig. 3). The distance between the phosphate groups in the major groove of a DNA/DNA duplex is twice that in an RNA/RNA duplex. Therefore, none of the peptides were able to interact with the DNA/DNA duplexes. In the minor groove of a DNA/DNA duplex, the interstrand phosphate groups are much closer than those in the major groove. However, the phosphate groups facing outward of the minor groove are unfavorable to form hydrogen bonds with the protonated amino groups of cationic peptides.

The peptides with guanidino groups (**5**, **6**, **7**) exhibited the same tendency as the peptides with the amino groups (Fig. 4, Table 2) for the RNA/RNA duplexes. Peptides with shorter side chain lengths had higher T_m values. This result indicates that the position of guanidino groups in Agp_8 (**5**) also fits well with the RNA duplex structure. While the distance between the functional groups is similar in the peptides with amino and guanidino groups, the peptides with

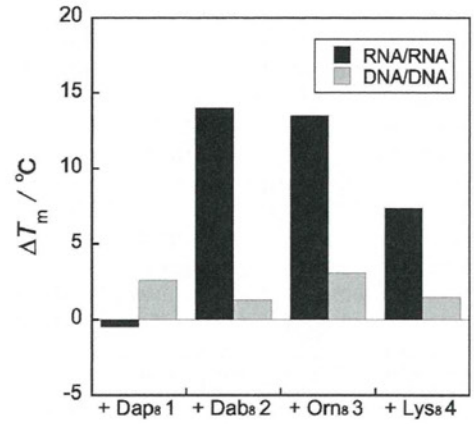

Figure 3. Melting temperature enhancements for the RNA/RNA and DNA/DNA duplexes at pH 7.0 in the presence of peptides **1**–**4**. Differences in the thermal melting points (ΔT_m) are given for the nucleic acid duplexes in the presence of equimolar amounts of peptide relative to the duplex alone. The dark gray columns represent ΔT_m for RNA/RNA duplex, and light gray columns represent ΔT_m values for DNA/DNA duplex.

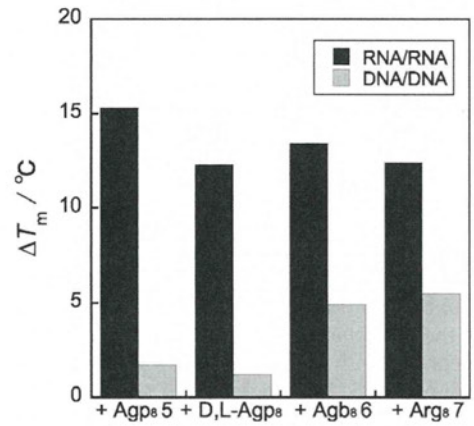

Figure 4. Melting temperature enhancements for the RNA/RNA and DNA/DNA duplexes at pH 7.0 in the presence of peptides **5**–**7**. Differences in the thermal melting points (ΔT_m) are given for the nucleic acid duplexes in the presence of an equal amount of peptide relative to the duplex alone. The dark gray columns represent ΔT_m for RNA/RNA duplex, and light gray columns represent ΔT_m values for DNA/DNA duplex.

Table 2
Thermal melting points (T_m in °C) for oligonucleotide duplex (in the absence and presence of peptides with guanidino groups[a])[b]

Peptide	RNA/RNA	ΔT_m	DNA/DNA	ΔT_m
None	60.7		48.2	
Agp_8	76.9	16.2	49.9	1.7
D-Agp_8	75.8	15.1	48.9	0.7
D,L-Agp_8	73.0	12.3	49.4	1.2
Agb_8	74.1	13.4	53.1	4.9
Arg_8	73.1	12.4	53.7	5.5

[a] Peptide concentration 4 μM.
[b] Buffer (10 mM phosphate buffere for pH 7.0), NaCl (100 mM), together with each oligonucleotide strand (4 μM). T_m values are reported at the means of duplicate measurements.

the guanidino groups exhibited higher T_m values. These different T_m values can be attributed to the different features of the functional groups. The guanidino group is known to have a stronger interaction with phosphate groups than amino groups, and thus the peptides with guanidino groups showed a stronger interaction

with the nucleic acid duplexes. However, in the case of the DNA/DNA duplex, the tendency changed because of the differences in the guanidino and amino functional groups. For the peptides with guanidine groups, those with longer side chain lengths had higher T_m values. This result may also be due to the fact that the guanidino groups strongly interact with the phosphate groups.

The different side chain lengths of the peptides resulted in different thermal stabilities of the nucleic acid duplexes. The duplex stability may also be affected by the flexibility of the peptides. Thus, to investigate the effect of incorporation of flexible residues into the peptide backbone, glycine was inserted into Agp_8 (**5**) to increase the flexibility of the main chain (**8**, **9**, **10**). Interestingly, it was found that an increase in the flexibility of the main chain did not affect the thermal stability of the peptide–RNA complexes (Fig. 5, Table 3). These results suggest that the stabilization of the RNA duplex with Agp_8 (**5**) is mainly attributed to enthalpic factors. In addition, insertion of L-alanine (Ala) or L-proline (Pro) into Agp_8 (**5**) also did not affect the thermal stability of the RNA duplexes (**11**, **12**). If the peptides invade the major groove, the redundant amino acid residues will give rise to steric hindrance and decrease the thermal stability. Therefore, these results suggest that the peptides interact with the surface of the nucleic acids.

Peptides with alternate arrangements also did not stabilize the RNA duplexes (Fig. 6, Table 4). Peptides consisting of Agp and Gly in an alternate arrangement, AgpG (**13**) did not have any effects on the RNA/RNA duplex. On the other hand, Agp_4 showed an appreciable stabilization effect for the RNA/RNA duplex. Therefore, a consecutive Agp sequence is effective for RNA/RNA duplex stabilization. Furthermore, Agp_8G3 (**10**), in which four Agp_2 units are connected, has the same affinity as Agp_8; thus, the Agp_2 structural unit is effective for the interaction with RNA/RNA duplexes. In Agp oligomers with a consecutive sequence, the guanidino groups are located on both sides of the peptide backbone, and this alignment is identical to that required for interaction between the guanidino groups and the phosphates in the major groove of RNA duplexes. However, peptides with a combination of guanidino and hydroxy or amide groups (AgpS (**14**) and AgpN (**15**), respectively) had no effects on the thermal stability of RNA duplexes. These results also suggest that a consecutive arrangement of cationic amino acids is essential for effective interaction with the phosphates of RNA duplexes.

The effect of chirality was also examined. The Agp oligomers consisting of all-L- and all-D-amino acids had similar T_m values,

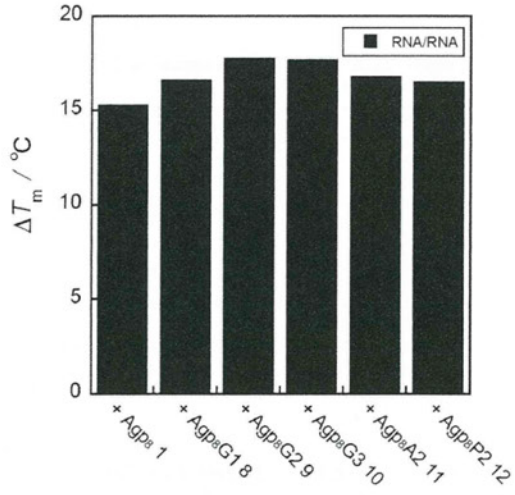

Figure 5. Melting temperature enhancements for the RNA/RNA duplexes at pH 7.0 in the presence of peptides **1**, **8**–**12**. Differences in the thermal melting points (ΔT_m) are given for the nucleic acid duplexes in the presence of an equal amount of peptide relative to the duplex alone.

Table 3
Thermal melting points (T_m in °C) for oligonucleotide duplex (in the absence and presence of peptides with flexible main chian[a])[b]

Peptide	RNA/RNA	ΔT_m
None	60.9	
Agp_8	77.5	16.6
Agp_8G1	77.5	16.6
Agp_8G2	78.8	17.9
Agp_8G3	78.6	17.7
Agp_8A2	77.7	16.8
Agp_8P2	77.4	16.5

[a] Peptide concentration 4 μM.
[b] Buffer (10 mM phosphate buffere for pH 7.0), NaCl (100 mM), together with each oligonucleotide strand (4 μM). T_m values are reported at the means of duplicate measurements.

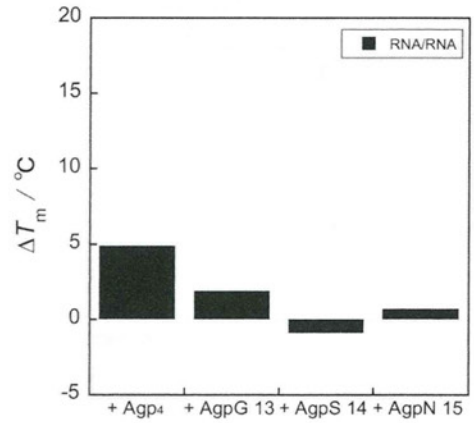

Figure 6. Melting temperature enhancements for the RNA/RNA duplexes at pH 7.0 in the presence of peptides **13**–**15**. Differences in the thermal melting points (ΔT_m) are given for the nucleic acid duplexes in the presence of equimolar amounts of peptide relative to the duplex alone.

Table 4
Thermal melting points (T_m in °C) for oligonucleotide duplex (in the absence and presence of peptides with alternate arrangements[a])[b]

Peptide	RNA/RNA	ΔT_m
None	60.3	
Agp_4	65.2	4.9
AgpG	62.2	1.9
AgpS	58.9	−1.4
AgpN	60.5	0.2

[a] Peptide concentration 4 μM.
[b] Buffer (10 mM phosphate buffere for pH 7.0), NaCl (100 mM), together with each oligonucleotide strand (4 μM). T_m values are reported at the means of duplicate measurements.

but the peptides having D/L-alternate arrangements slightly had lower thermal stability. A decrease in the thermal stability induced by a heterochiral backbone was also reported for chiral PNA.[16]

2.3. CD spectroscopy

The structures of the peptides and the RNA–peptide complexes in solution were analyzed using circular dichroism (CD) spectroscopy. On the basis of molecular mechanics calculations,[15] the amino groups and guanidino groups of the peptides, particularly in Dap_8 (**2**) and Agp_8 (**5**), can form intramolecular hydrogen bonds with the amido groups in the main chain. However, in the absence of nucleic acid duplexes, the spectra of all the peptides indicated the presence of random coils.[17] Therefore, the effect of the secondary structures of the peptides was negligible in these cases. The

structures of the RNA–peptide complexes were also analyzed. Because the peptides showed a variety of T_m values depending on the side chain length and the nature of the cationic functional groups, there existed not only electrostatic interactions and hydrogen bonding, but also structural factors. However, for both the RNA and DNA duplexes, no appreciable structural changes in the nucleic acids were observed following the addition of the peptides (Figs. 7 and 8). The CD spectra of the RNA and DNA duplexes in the presence and absence of peptides were typical for A-type and B-type helices, respectively.

2.4. ITC measurement

Thermodynamic analysis of the peptide–nucleic acid interactions was carried out using isothermal titration calorimetry (ITC) measurements. The duplex concentration was 2.5 times higher than that used for the UV melting analyses because the amount of heat generated during the binding between the nucleic acid duplexes and the oligocationic peptides was expected to be insufficient for calculation of the thermodynamic parameters at the lower concentration. Figures 9, S8,[17] and S9[17] show the preliminary results for the ITC titration of the peptides with the self complementary RNA/RNA duplex r(CGCGAAUUCGCG)$_2$ and DNA/DNA duplex d(CGCGAATTCGCG)$_2$. In addition to electrostatic interactions and hydrogen bonding between the peptides and nucleic acids, dehydration and dissociation of the phosphates in the buffer solution were apparently observed. Thus, the interactions were too complex for calculation of the thermodynamical parameters. However, it was observed that both of the peptides selectively interacted with the RNA/RNA duplexes. In contrast, only Agb_8 (**5**) interacted with both the RNA/RNA and DNA/DNA duplexes. This result may be due to the fact that, in Agb_8, the side chain is long and sufficiently flexible to interact with the phosphate groups of both the RNA/RNA and DNA/DNA duplexes. In comparison with the amino-substituted Dap_8, the guanidine-substituted Dab_8 (**5**) had larger endothermic interactions.

Inhibition assays were carried out to clarify the peptide-binding sites in the RNA duplexes. The peptides were titrated into a solution of the RNA duplexes in the presence of neomycin, which is known to bind to the major groove of RNA duplexes.[18] The inhibition of peptide–RNA binding by neomycin was different for the types of peptides (Fig. S10[17]). For Dab_8 (**2**), the exothermic interactions were selectively inhibited, while the endothermic interactions were still observed. On the other hand, for Agp_8 (**5**), both of the interactions were inhibited. These results suggest that the exothermic interactions are attributed to the binding of the peptides to the major groove of RNA/RNA duplexes and the endothermic interactions are related to the interactions with other sites.

3. Materials and methods

3.1. Peptide synthesis

Peptides were synthesized via a conventional solid-phase method by using the 9-fluorenylmethyloxycarbonyl (Fmoc) strategy.[19] The peptide chains were assembled on a Fmoc-NH-SAL-PEG resin by using Fmoc amino acid derivatives (5 equiv), *N*,*N*-diisopropylethylamine (DIPEA, 10 equiv), and 2-(1*H*-9-azabenzotriazole-1-yl)-1,1,3,3-tetramethyluronium hexafluorophosphate (HATU, 5 equiv) in dimethylformamide (DMF) for the coupling, and 25% piperidine/DMF for the removal of the Fmoc group. After coupling of the last amino acids, amino groups at the N-termini were protected with an acetyl (Ac) group using acetic anhydride (10 equiv). To cleave the peptide from the resin and remove the side chain protecting groups, the peptide resin was treated with trifluoroacetic acid (TFA)-triisopropylsilane-water, (95:2.5:2.5, v/v/v). Peptides in sat $NaHCO_{3aq}$ (200 μl) were added in one portion to a solution of the 1,3-di-Boc-2-(trifluoromethylsulfonyl)guanidine[20] (10 equiv per amino groups) in dioxane (200 μl), and stirred overnight at rt, then concentrated in vacuo. To remove the protecting groups from the guanidino groups, the peptides were treated with TFA–triisopropylsilane–water (95:2.5:2.5, v/v/v). All peptides were purified with reverse-phase HPLC (0.05% TFA in water–acetonitrile). The peptides were successfully identified by matrix-assisted laser desorption ionization time-of-flight mass spectrometry (MALDI-TOF-MS). Compound **1**, TOF-MS *m*/*z* calcd for $[M+Na]^+$ 1048.07; Found 1047.60. Compound **2**, TOF-MS *m*/*z* calcd for $[M+H]^+$ 1138.31; Found 1137.22. Compound **3**, TOF-MS *m*/*z* calcd for $[M+Na]^+$ 1272.50; Found 1271.56. Compound **4**, TOF-MS *m*/*z* calcd for $[M+H]^+$ 1362.73; Found 1361.51. Compound **5**, TOF-MS *m*/*z* calcd for $[M+H]^+$ 1362.41; Found 1361.51. Compound **6**, TOF-MS *m*/*z* calcd for $[M+H]^+$ 1474.63; Found 1473.77. Compound **7**, TOF-MS *m*/*z* calcd for $[M+H]^+$ 1586.84; Found 1585.72. Compound **8**, TOF-MS *m*/*z* calcd for $[M+H]^+$ 1419.46; Found 1418.53. Compound **9**, TOF-MS *m*/*z* calcd for $[M+Na]^+$ 1476.52; Found 1476.00. Compound **10**, TOF-MS *m*/*z* calcd for $[M+H]^+$ 1533.57; Found 1533.07. Compound **11**, TOF-MS *m*/*z* calcd for $[M+H]^+$ 1504.57; Found 1504.21. Compound **12**, TOF-MS *m*/*z* calcd for $[M+H]^+$ 1556.64; Found 1555.68. Compound **13**, TOF-MS *m*/*z* calcd for $[M+Na]^+$ 1100.07; Found 1099.25. Compound **14**, TOF-MS *m*/*z*

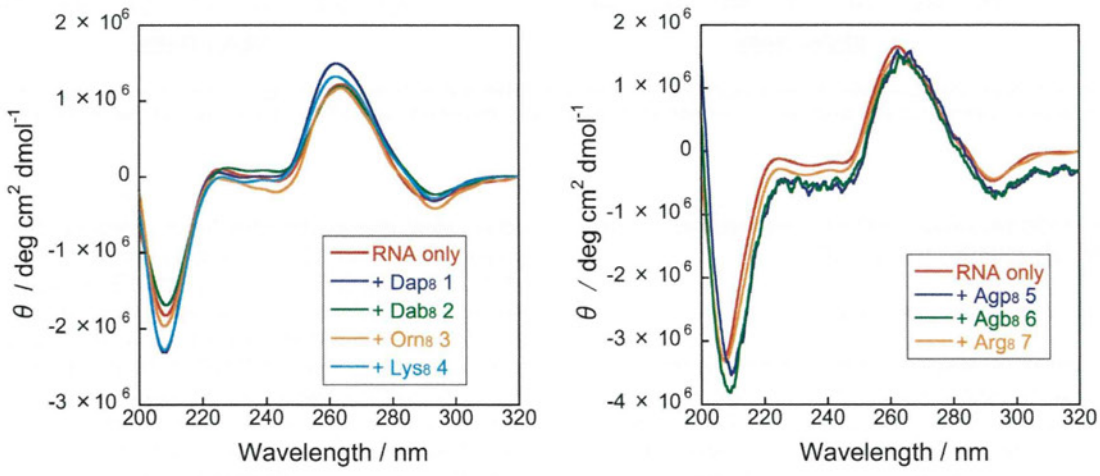

Figure 7. CD spectra of the RNA/RNA duplexes in the presence and absence of an equal amount of peptides **1–7** (at 20 °C, pH 7.0, 4 μM each of peptide and duplex).

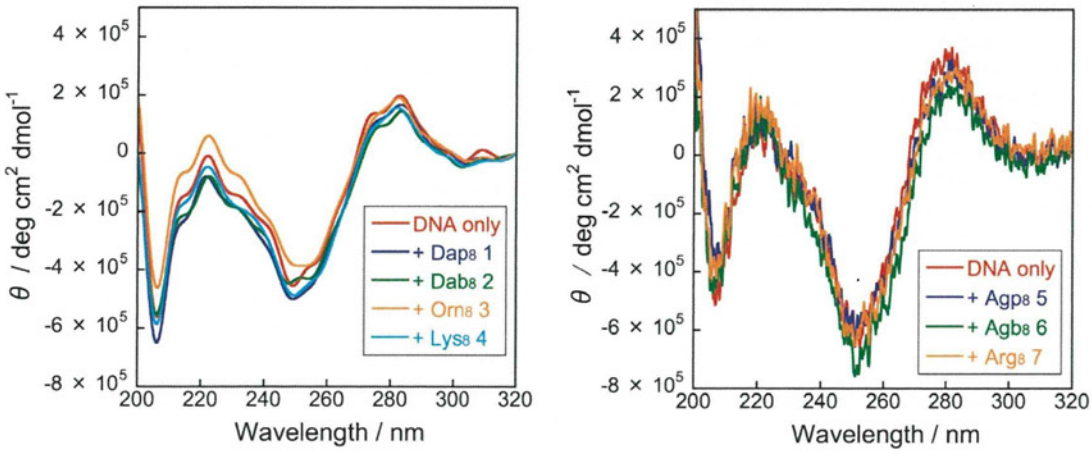

Figure 8. CD spectra of the DNA/DNA duplexes in the presence and absence of an equal amount of peptides **1–7** (at 20 °C, pH 7.0, 4 μM each of peptide and duplex).

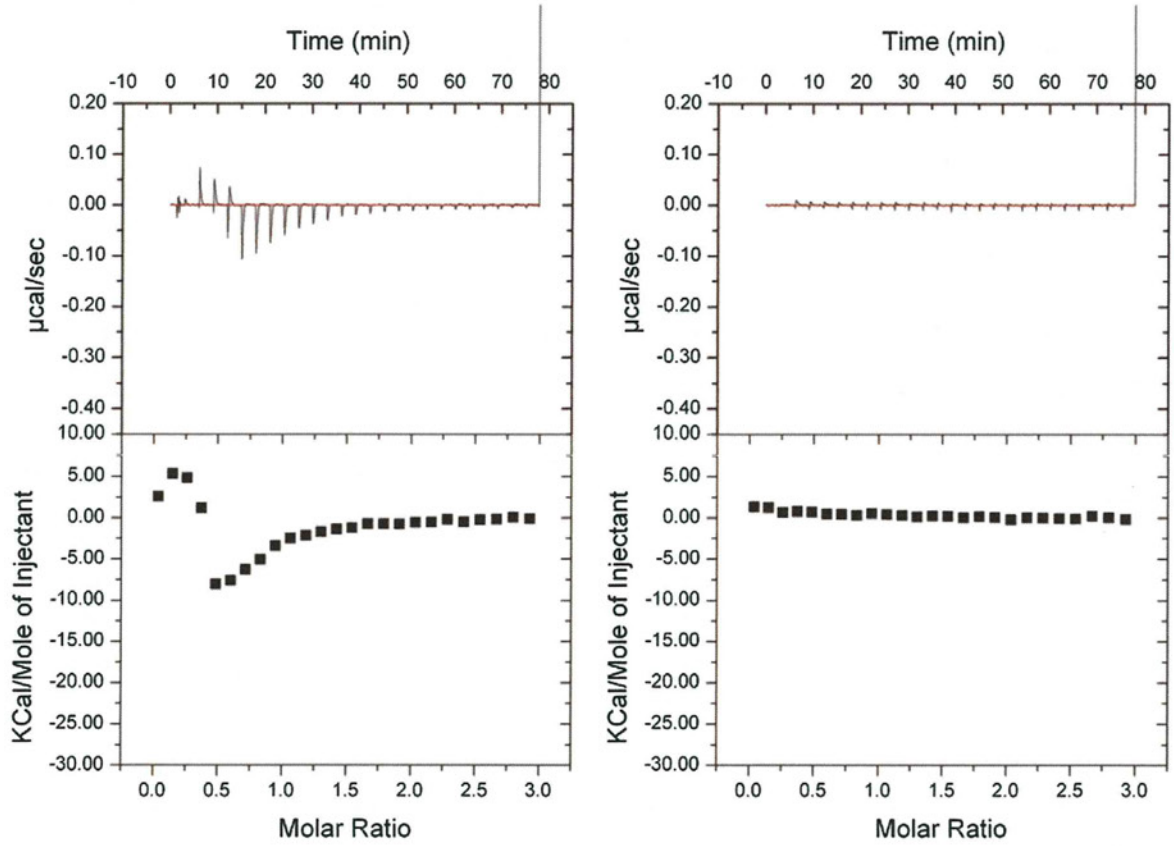

Figure 9. ITC profiles at 25 °C for titration of Dab_8 (**2**) into a solution of RNA/RNA duplex (left) and DNA/DNA duplex (right); each curve is the result of a 2.5 μl injection of 150 μM peptide. The duplex concentration was 10 μM in a 10 mM phosphate buffer with 100 mM NaCl at pH 7.0; corrected injection heat in the cases of RNA/RNA were plotted.

calcd for $[M+H]^+$ 1198.18; Found 1197.67. Compound **15**, TOF-MS *m/z* calcd for $[M+H]^+$ 1306.29; Found 1305.46.

3.2. Melting temperature (T_m) analysis

Absorbance versus temperature profile measurements were carried out in quartz cells with a 1 cm path length using an eight-sample cell changer. The variation in the UV absorbance with temperature was monitored at 260 nm. The temperature was scanned from 10 to 95 °C at a rate of 0.2 °C/min. The peptides were added after oligonucleotides were annealed. The samples were prepared as follows. The oligonucleotides were dissolved in a phosphate buffer (10 mM) containing NaCl (0.1 M) at pH 7.0. The solutions of oligonucleotides (4 μM) were first rapidly heated to 95 °C, left for 10 min, and then cooled to 10 °C at a rate of 1 °C/min. The equal amounts of peptides (final concn: 4 μM) were then added to the solution. The samples were left to equillbrate at the starting temperature for 30 min, the dissociation of the duplex was observed by heating the solution to 95 °C at a rate of 0.2 °C/min, and data points were collected at every 0.1 °C.

3.3. CD spectroscopy

All CD spectra were recorded at 20 °C. The following instrument settings were used: resolution, 0.1 nm; sensitivity, 10 mdeg; response, 4 s; speed, 10 nm/min; accumulation, 6.

3.4. Conditions for ITC experiments

The peptides and nucleic acid duplexes were dissolved in a 10 mM phosphate buffer containing 100 mM NaCl at pH 7.0. The peptide solutions (150 μM) were titrated into the nucleic acid duplex solutions (10 μM) at 25 °C. Each titration of peptide solution consisted of a preliminary 0.5 μl injection followed by 24 subsequent 1.5 μl additions, which were performed over 3 s periods at 120 s intervals. In the inhibition assays, the peptide solutions were titrated into the nucleic acid solution in the presence of 100 μM neomycin under the same conditions as described above.

4. Conclusion

We have synthesized a series of cationic oligopeptides by systematically changing the position of the cationic groups. On the basis of UV-melting analysis, CD spectrometry and ITC measurements, these cationic oligopeptides showed different tendencies for the stabilization of nucleic acid duplexes. Peptides with amino groups stabilized only RNA duplexes, while peptides with guanidino groups stabilized both RNA and DNA duplexes. In particular, Dab_8 (**2**) and Agp_8 (**5**) showed the highest T_m values among the series of peptides with the same cationic groups but different side chain length. These results suggest that the distance between the cationic groups, such as in Dab_8 (**2**) and Agp_8 (**5**), are well fitted to the distance between the phosphate groups in the major groove of RNA duplexes. Furthermore, peptides with alternate arrangements and those containing flexible amino acids did not stabilize the RNA duplexes. These results indicate that at least two consecutive sequences of Agp are necessary for effective binding of cationic oligopeptides to RNA duplexes. Therefore, given their unique properties, Dab_8 (**2**) and Agp_8 (**5**) will be useful as stabilizers of dsRNA-based nucleic acid drugs or new materials for their DDS.

Acknowledgments

We thank Professor Kohei Tsumoto (University of Tokyo) and Dr. Satoru Nagatoishi (University of Tokyo) for the ITC measurements and helpful discussions. This work was finally supported by KAKENHI and CREST, the Japan Science and Technology Agency.

Supplementary data

Supplementary data (data include CD spectra, UV melting profiles, and ITC profiles) associated with this article can be found, in the online version, at http://dx.doi.org/10.1016/j.bmc.2013.01.053.

References and notes

1. Fire, A.; Xu, S.; Montgomery, M. K.; Kostas, S. A.; Driver, S. E.; Mello, C. C. *Nature* **1998**, *391*, 806.
2. Watts, J. K.; Deleavey, G. F.; Damha, M. J. *Drug Discovery Today* **2008**, *13*, 842.
3. (a) Manoharan, M. *Biochim. Biophys. Acta* **1999**, *1489*, 117; (b) Cook, P. D. *Nucleosides Nucleotides* **1999**, *18*, 1141.
4. Eguchi, A.; Meade, B. R.; Chang, Y. C.; Fredrickson, C. T.; Williert, K.; Puri, N.; Dowdy, S. F. *Nat. Biotechnol.* **2009**, *27*, 567.
5. Prakash, T. P.; Allerson, C. R.; Vickers, T. A.; Sioufi, N.; Jarres, R.; Baker, B. F.; Swayze, E. E.; Griffey, R. H.; Bhat, B. *J. Med. Chem.* **2005**, *48*, 4247.
6. Francois, B.; Russell, R.; Murray, J. *Nucleic Acids Res.* **2005**, *33*, 5677.
7. Maris, C.; Dominguez, C.; Allain, F. H. *FEBS J.* **2005**, *272*, 2118.
8. (a) Nurtola, M.; Zaramella, S.; Yeheskiely, E.; Strömberg, R. *ChemBioChem* **2010**, *11*, 2606; (b) Wu, C. H.; Chen, Y. P.; Mou, C. Y.; Cheng, R. P. *Amino Acids* **2012**. http://dx.doi.org/10.1007/s00726-012-1357-0.
9. Iwata, R.; Sudo, M.; Nagafuji, K.; Wada, T. *J. Org. Chem.* **2011**, *76*, 5895.
10. Lemberg, M. K.; Martoglio, B. *Mol. Cell* **2002**, *10*, 735.
11. Futaki, S.; Suzuki, T.; Ohashi, W.; Yagami, T.; Tanaka, S.; Ueda, K.; Sugiura, Y. *J. Biol. Chem.* **2001**, *276*, 5836.
12. Kim, S. W.; Kim, N. Y.; Choi, Y. B.; Yang, J. M.; Shin, S. *J. Controlled Release* **2010**, *143*, 334.
13. Russell, A. L.; Williams, B. C.; Spuches, A.; Klapper, D.; Srouji, A. H.; Hicks, R. P. *Bioorg. Med. Chem.* **2012**, *20*, 1723.
14. Jones, S.; Daley, D. T.; Luscombe, N. M.; Berman, H. M.; Thornton, J. M. *Nucleic Acids Res.* **2001**, *29*, 943.
15. Mohamadi, F.; Richards, N. G. J.; Guida, W. C.; Liskamp, R.; Lipton, M.; Caufield, G.; Chang, G.; Hendrickson, T.; Still, W. C. *J. Comput. Chem.* **1990**, *143*, 334.
16. Ura, Y.; Leman, J.; Orgel, L. E.; Ghadiri, M. R. *Science* **2009**, *325*, 73.
17. See the Supplementary data.
18. Varani, L.; Spillantini, M. G.; Goedert, M.; Varani, G. *Nucleic Acids Res.* **2000**, *28*, 710.
19. *Fmoc Solid Phase Peptide Synthesis*; Chan, W. C., White, P. D., Eds.; Oxford University Press: New York, 2000. pp 42–76.
20. Xiao, S.; Fu, N.; Peckham, K.; Smith, B. D. *Org. Lett.* **2010**, *12*, 140.

JOC The Journal of Organic Chemistry

Article

pubs.acs.org/joc

Stereocontrolled Solid-Phase Synthesis of Phosphorothioate Oligoribonucleotides Using 2′-*O*-(2-Cyanoethoxymethyl)-nucleoside 3′-*O*-Oxazaphospholidine Monomers

Yohei Nukaga,[†] Kohei Yamada,[‡] Toshihiko Ogata,[†] Natsuhisa Oka,[§] and Takeshi Wada*[,†]

[†]Department of Medical Genome Sciences, Graduate School of Frontier Sciences, The University of Tokyo, Bioscience Building 702, 5-1-5 Kashiwanoha, Kashiwa, Chiba 277-8562, Japan

[‡]Yamasa Corporation, 10-1 Araoi-cho 2-chome, Choshi, Chiba 288-0056, Japan

[§]Department of Chemistry, Faculty of Engineering, Gifu University, Yanagido 1-1, Gifu 501-1193, Japan

Supporting Information

ABSTRACT: A method for the synthesis of *P*-stereodefined phosphorothioate oligoribonucleotides (PS-ORNs) was developed. PS-ORNs of mixed sequence (up to 12mers) were successfully synthesized by this method with sufficient coupling efficiency (94−99%) and diastereoselectivity (≥98:2). The coupling efficiency was greatly improved by the use of 2-cyanoethoxymethyl (CEM) groups in place of the conventional TBS groups for the 2′-*O*-protection of nucleoside 3′-*O*-oxazaphospholidine monomers. The resultant diastereopure PS-ORNs allowed us to clearly demonstrate that an ORN containing an all-(*Rp*)-PS-backbone stabilizes its duplex with the complementary ORN, whereas its all-(*Sp*)-counterpart has a destabilizing effect.

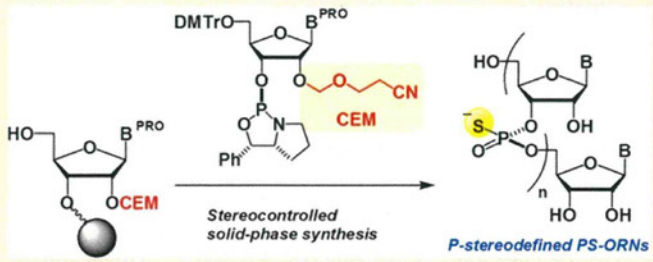

INTRODUCTION

Post-transcriptional gene silencing, mediated by RNA molecules such as short interfering RNAs (siRNAs) and microRNAs (miRNAs), has been extensively studied for its therapeutic potential in treating various diseases.[1] Conversely, miRNA itself has also emerged as a potential therapeutic target owing to its susceptibility to being silenced by antisense oligonucleotides.[2] In addition, gene silencing by siRNA has become a powerful tool for functional genomics.[3] Synthetic oligoribonucleotides (ORNs) with appropriate chemical modifications are useful for these applications, especially for therapeutic purposes that require oligonucleotides with sufficient nuclease stability, cell membrane permeability, and favorable pharmacokinetic properties.[1,2] Among various chemically modified ORN analogues developed so far, phosphorothioate oligoribonucleotide (PS-ORN) is one of the most well studied analogues owing to its sequence-specific hybridizing affinity for target RNAs and water solubility, features that are comparable to those of natural ORNs, as well as its high nuclease stability and lipophilicity.[1]

A PS-ORN has chiral phosphorus atoms, and its properties are theoretically dependent on the configuration of these phosphorus atoms because it functions by interacting with chiral biomolecules such as nucleic acids and proteins.[4] For this reason, efforts have been made to develop methods for synthesizing *P*-stereodefined PS-ORNs.[4b,5] For example, ORNs containing a single stereodefined PS-linkage at a specific position have often been prepared by chromatographic separation of diastereomixtures[6] and used as probes to study the functions of the pro-*Rp* and pro-*Sp* oxygen atoms of the corresponding phosphodiesters in various RNA-related biological processes.[4] However, this method is not applicable to the preparation of ORNs with multiple stereodefined PS-linkages, which are required for therapeutic studies. Diastereopure dimer building blocks can be used to incorporate multiple stereodefined PS-linkages into ORNs; however, this method requires up to 32 types of building blocks (four types of nucleosides for each of the 3′- and 5′-nucleosides and two *P*-diastereomers) and yet cannot produce ORNs having consecutive stereodefined PS-linkages.[7a,b] *P*-Stereodefined PS-ORNs can also be synthesized using RNA polymerases, but only those with (*Rp*)-PS-linkages are available, and this method is not suitable for large-scale syntheses.[7c,8] Although chemical syntheses of *P*-stereodefined PS-ORNs using stereoselective or stereospecific reactions have also been studied, the methods reported to date suffer from low coupling efficiency or stereoselectivity.[9−11] Recently, an siRNA duplex having four consecutive (*Rp*)-PS-linkages at both ends has been synthesized using chromatographically separated diastereopure nucleoside 3′-phosphorothioate triester derivatives as monomers.[12] To the best of our knowledge, this is the only report in the literature describing the chemical synthesis of *P*-stereodefined PS-ORNs longer than 3mers with sufficient stereo-

Received: June 7, 2012
Published: August 29, 2012